Chemical Engineering Journal 536 (2026) 175798

Contents lists available at ScienceDirect

Chemical Engineering Journal

journal homepage: www.elsevier.com/locate/cej

Unraveling the effect of alkaline recovery conditions on the complexity and diversity of extracellular polymeric substances (EPS) from aerobic granular sludge towards effective waste-to-value strategies in wastewater treatment

Benedetta Pagliaccia [a,*], Yuemei Lin [b], Emiliano Carretti [c,d], Lucrezia Caselli [c,d], Claudio Lubello [a], Tommaso Lotti [a]

[a] Department of Civil and Environmental Engineering, University of Florence, Via di Santa Marta 3, 50139, Florence, Italy
[b] Department of Biotechnology, Delft University of Technology, Van der Maasweg 9, 2629, HZ, Delft, the Netherlands
[c] Department of Chemistry "Ugo Schiff", University of Florence, Via della Lastruccia 3, 50019, Sesto Fiorentino, Florence, Italy
[d] Center for Colloid and Surface Science – CSGI, Via della Lastruccia 3, 50019, Sesto Fiorentino, Florence, Italy

ARTICLE INFO

Keywords:
Extracellular polymeric substances
Alkaline extraction
Hydrogels
Rheology
Small-angle X-ray scattering
Resource recovery

ABSTRACT

Extracellular polymeric substances (EPS) are essential for the structural and functional stability of aerobic granular sludge (AGS). Their complexity makes comprehensive characterization challenging and dependent on the recovery approach. This study thus investigates how alkaline extraction conditions influence the recoverability and properties of AGS-derived EPS, especially regarding structural EPS (sEPS) and related hydrogels. An advanced methodological framework was applied to compare NaOH- and Na_2CO_3-based extractions through a holistic assessment of multi-scale characterization data. The biochemical composition, molecular weight distribution and thermal behavior of EPS and/or sEPS were studied by complementary techniques (e.g. methods for protein/carbohydrate determination, size exclusion chromatography and thermogravimetry). An innovative physicochemical approach coupling small-angle X-ray scattering (SAXS) and rheology was employed to investigate the nano-scale arrangements and mechanical features of sEPS hydrogels. The NaOH-based extraction resulted in lower EPS/sEPS yields, promoting a shift towards lower molecular weight sEPS fractions. The Na_2CO_3-based method preserved larger and more thermally resistant macromolecules, suggesting milder chemical effects on the recovered EPS/sEPS. SAXS revealed that the sEPS hydrogel network consisted of 3D mass fractals and highly ordered lamellar, multilayered domains – more pronounced for Na_2CO_3-based protocol – potentially associated with lipopolysaccharide assemblies. NaOH-extracted sEPS formed stiffer hydrogels. The NaOH-based protocol likely induced harsher hydrolysis/partial degradation of specific EPS constituents (e.g. large proteins and lipidic fractions), which may not significantly contribute to, or even compromise, the hydrogel stiffness. Overall, this work demonstrates the critical role of alkaline extraction in determining EPS/sEPS yield and properties, providing valuable insights for the rational design of EPS-based biomaterials and recovery strategies.

1. Introduction

In the field of environmental biotechnology, particularly in the context of wastewater treatment, increasing attention is being paid to extracellular polymeric substances (EPS) from the perspectives of both bioprocess engineering and resource recovery. EPS are a complex mixture of biopolymers, mainly comprising polysaccharides, proteins and other constituents such as lipids and humic-like substances [1–3]. In all biofilms, microorganisms are embedded in a matrix of hydrated EPS, mostly produced by the microorganisms themselves [1]. EPS largely participate in the formation and stability of biofilms: they contribute to initial adhesion/aggregation of cells and provide structural integrity, protection and other functional properties to microbial aggregates [1–3]. Despite the huge effort made in recent years to solve the composition and structure of EPS, there is still a lack of knowledge regarding their fine characterization. The high complexity and diversity

* Corresponding author.
E-mail addresses: benedetta.pagliaccia@unifi.it (B. Pagliaccia), Yuemei.Lin@tudelft.nl (Y. Lin), emiliano.carretti@unifi.it (E. Carretti), lucrezia.caselli@unifi.it (L. Caselli), claudio.lubello@unifi.it (C. Lubello), tommaso.lotti@unifi.it (T. Lotti).

https://doi.org/10.1016/j.cej.2026.175798
Received 18 December 2025; Received in revised form 30 March 2026; Accepted 31 March 2026
Available online 1 April 2026

of EPS, together with the challenges in isolating and processing key EPS components, hinders a comprehensive understanding of their structure, composition and functionality, pointing out the need for more advanced and integrated approaches [3]. Depending on the method applied to extract EPS and measure their major constituents, the quantification and characterization of EPS fractions can vary, thus hindering a consistent comparison among literature data. However, there is a consensus that proteins (PN) and carbohydrates (PS) are among the main EPS components [2,4]. Colorimetric methods commonly applied to measure PN and PS in EPS are generally considered reference techniques for cross-comparison among scientific studies, providing an overall assessment of the EPS biochemical composition. However, the outcome of these analyses is strictly dependent on the selected standard compounds and prone to interference from other EPS components [5]. Moreover, these approaches alone do not allow the detection of individual EPS constituents. A combination of improved analytical methods and possibly the use of a broader suite of fluorescence-binding proteins coupled with microscopy enabled significant progress towards better resolution of EPS characterization [6], leading to the identification of specific constituents such as glycoproteins [7], amyloids [8,9], sialic acids [10], hyaluronic acid-like and sulfated glycosaminoglycans-like polymers [11].

Elucidating the composition and properties of EPS not only enables greater control of chemistry and biology in bioprocess engineering but also increases opportunities for sustainable resource recovery and circular bioeconomy. Thanks to their versatile properties, EPS are recognized as a valuable resource for the development of highly effective biomaterials such as flame retardant [12] and water-proof coating [13] for textile and paper industries, adsorbent media [14,15] and flocculants [16] in wastewater treatment, functionalized products for sustainable agronomic practices [17] and additives for cement curing in construction sector [18]. The recovery of EPS from waste sludge allows not only to yield valuable biomaterials but also to reduce the mass of sludge to be handled, thus potentially increasing the overall environmental and economic sustainability of wastewater treatment.

Due to the development of aerobic granular sludge (AGS) technologies, large research interest was devoted in recent years to the recovery and industrial valorization of AGS-extracted EPS. Among the advantages of AGS processes (such as better settling properties, simultaneous carbon, nitrogen and phosphorus removal, more compact treatment facilities, etc. [19,20]), a high potential for resource recovery, including EPS, is evidenced. With respect to conventional activated sludge (CAS), waste AGS can be concentrated by simple draining up to about 11 wt% thanks to its dense granular structure, providing a concentrated feedstock for downstream recovery processes [17]. AGS-derived EPS exhibit peculiar physicochemical properties that make them suitable for the design of high-value biomaterials. Of interest is the feasibility of forming ionically cross-linked hydrogels with solid-like rheological features and high water-holding capacity [17,21–25]. Within the scientific community, the hydrogel-forming capacity is usually associated with a subset of EPS that are referred to as structural EPS (sEPS) due to their primary contribution to the formation of the tertiary network structure and thus to the structural integrity of microbial aggregates [22]. Differences in the hydrogel-forming behavior of CAS- and AGS-derived EPS have been linked to their distinct chemical structure. Specifically, EPS from AGS have been reported to form self-standing hydrogels with superior rheological properties compared to EPS from CAS. Lin et al. [26] attributed the enhanced hydrogel-forming capacity and post-gelling mechanical features of AGS-derived EPS to their higher relative content of poly(guluronic acid) blocks (GG-blocks). More recently, Li et al. [27] stated that the differences in the composition and structure of lipopolysaccharides (LPS) from CAS and AGS (e.g. inverted structures with the water phase in between versus bilaminar multilayered arrangements in LPS-Ca aggregates) may also play a crucial role. The hydrogels formed by AGS-derived sEPS were primarily studied by mechanical testing [21,23–26,28,29]. A lower number of contributions employed complementary techniques, such as microscopy [25] and thermogravimetric analysis [23], or experimental approaches aimed to address other relevant physicochemical properties (e.g. swelling capacity [17]). However, the structural characteristics of AGS-derived sEPS hydrogels at nano-scale level are still poorly investigated. A comprehensive understanding of the structural and functional features of sEPS hydrogels is useful to fully exploit their applicative potential. Advancing knowledge in this area would thus facilitate the development of sEPS hydrogels tunable for specific uses. These bio-based materials may contribute to increase the overall environmental sustainability of industrial sectors currently dominated by synthetic polymeric products.

To characterize EPS and explore their applicative potential, it is typically necessary to extract them from sludge samples. To this aim, extraction methods based on physical approaches (e.g. centrifugation [30], heating [30–32] and sonication [22,30,33]), chemical protocols (using acids [33], ethylenediaminetetraacetic acid (EDTA) [22,30,33], cation exchange resins (CER) [30,33], etc.) and biological processes (enzymatic treatments [34]) are generally applied individually or in combination. These methods are characterized by distinct mechanisms, recovery efficiencies and impacts on cell lysis and polymer integrity [35]. Chemical protocols typically enable higher recovery yields than physical extractions [2,35] and can provide lower degrees of cell lysis and EPS degradation than some biological approaches [35]. Among these, EDTA- and CER-based methods are reported to be effective in minimizing the release of intracellular polymers when extracting EPS [2] but could be expensive and generally less feasible on industrial scale [36]. In recent years, physicochemical methods based on alkaline extraction (eventually coupled with heating) followed by acidic precipitation have gained increasing attention due to their effectiveness in recovering EPS/sEPS suitable for both characterization studies and downstream valorization processes [9,13,22,29,36]. Focusing on EPS from AGS, Felz et al. [22] proved that an alkaline extraction using Na_2CO_3, combined with heating and mixing, enhances EPS solubilization, leading to higher recovery yields compared to centrifugation, sonication, EDTA, formaldehyde + NaOH and formamide + NaOH methods. It is worth noting that even minor modifications in the recovery approach applied (e.g. in terms of chemicals and/or operative conditions) can influence the EPS/sEPS compositional and functional properties, such as molecular weight distribution, biochemical characterization, elemental composition, thermal behavior, etc. [17,29,36], with noticeable implications for both characterization and recovery purposes. Similarly, both EPS/sEPS extraction and hydrogel-forming protocols could affect the overall behavior and applicative effectiveness of sEPS hydrogels. In this regard, the effect of different recovery conditions (e.g. in terms of alkaline and acidic reagents such as NaOH/Na_2CO_3/K_2CO_3/$(NH_4)_2CO_3$ and HCl/HNO_3, respectively) and/or ionic cross-linking agents (e.g. Ca^{2+} – by using $CaCl_2$/$Ca(NO_3)_2{\cdot}4H_2O$/$Ca(C_2H_5COO)_2$ cross-linker solutions – or other divalent cations M^{2+}) was typically addressed in the literature with reference to a subset of chemicals/operating conditions and mainly focusing on mechanical properties [24,25,29], elemental composition [17] and swelling capacity [17].

Bearing in mind the above, a comprehensive characterization of EPS/sEPS and related hydrogels is therefore made challenging by their inherent complexity and diversity and further complicated by their high sensitivity to the extraction method adopted. Tailoring the recovery approach depending on the specific research objectives thus remains a central issue in EPS studies.

In this perspective, this study aims to get insights into the complex nature of AGS-derived EPS/sEPS and elucidate key structural and mechanical features of their hydrogels in response to different alkaline extraction conditions. Specifically, this work is primarily intended to verify a research hypothesis widely discussed within the scientific community, namely that the alkaline extraction chemistry plays a major role in determining the chemical composition and physicochemical characteristics of recoverable biopolymers, thus ultimately influencing

their overall functional properties. Such an extraction-driven effect is expected to cause changes in the supramolecular arrangements and mechanical features of the resulting sEPS hydrogels. In this regard, this study systematically compared different alkaline extraction strategies, exploring the reasons behind the different EPS/sEPS yields and properties typically observed in the case of physicochemical recovery approaches using sodium hydroxide (NaOH) instead of sodium carbonate (Na_2CO_3) as alkaline solubilization agent [29,36]. To this aim, a protocol widely adopted in the literature was selected as reference method for the EPS/sEPS extraction [22]. This well-established procedure couples a thermo-alkaline treatment, leading to higher EPS extraction yields compared to other chemical approaches, with a subsequent acidic precipitation stage for the recovery of the gel-forming EPS (or sEPS) [22]. While maintaining the same method operations, different extraction conditions were tested by alternatively using NaOH and Na_2CO_3 as alkaline reagents to solubilize the EPS matrix. The choice of applying NaOH- and Na_2CO_3-based protocols was guided by their literature relevance and proven effectiveness in EPS/sEPS recovery for fundamental and application-oriented investigations, thus allowing comparisons across different works [22,29,36]. An advanced methodological framework that combined multi-scale characterization data into a coherent system-level perspective was applied to compare NaOH- and Na_2CO_3-based extractions. This integrated approach helped to address the structural and functional complexity of the targeted EPS while shedding light on the critical role of extraction chemistry. The molecular weight distribution, biochemical composition and thermal behavior of the recovered EPS and/or sEPS were addressed by combining multiple techniques such as size exclusion chromatography (SEC), colorimetric methods for total protein (PN) and carbohydrate (PS) content determination and thermogravimetric and derivative thermogravimetric analysis (TGA-DTG). To get further insights, SEC-derived sEPS fractions were analyzed to evaluate their PN and PS concentrations and characterized by Fourier transform infrared (FT-IR) spectroscopy, while staining techniques were employed to visualize the presence and structure of lipopolysaccharides in the sEPS extracts. An innovative physicochemical, multi-scale approach integrating small-angle X-ray scattering (SAXS) and rheology was employed to synergistically investigate the supramolecular arrangements and mechanical features of ionically cross-linked sEPS hydrogels. By combining scattering-derived structural insights and rheological data, this approach would go beyond single-technique analyses, enabling a holistic assessment of sEPS hydrogel nano-scale assembly and mechanical behavior under different extraction conditions. Overall, this study allowed to elucidate key mechanistic relationships between EPS/sEPS extraction chemistry and resulting characterization, advancing fundamental knowledge on these complex and diverse systems. From an applicative perspective, the findings of this work would support the rational design of more efficient and targeted EPS/sEPS production chains while contributing to increase the yield, functionality and practical applicability of EPS-based biomaterials within the broader context of sustainable resource recovery.

2. Materials and methods

2.1. Extraction and hydrogel-formation

The extraction method developed by Felz et al. [22] was applied in this study with minor modifications in terms of chemicals and operative conditions used. While maintaining the same operational steps (i.e. thermo-alkaline extraction followed by acidic precipitation) proposed by Felz et al. [22], comparative extractions were conducted by alternatively using NaOH and Na_2CO_3 to solubilize the EPS matrix in the thermo-alkaline stage. To this aim, 200 μm-sieved AGS mixed liquor sludge was kept into 2 mM NaOH or 47 mM Na_2CO_3 aqueous solutions at a concentration of 0.12 g WW_{AGS}/mL (WW: Wet Weight) under stirred conditions (about 400 rpm) for 1 h at a controlled temperature of 80 °C. The temperature (80 °C), initial pH (~ 11.3) and Na_2CO_3 concentration (47 mM) adopted in this phase were selected to match those used in the reference method mentioned above [22]. Accordingly, the NaOH concentration (i.e. 2 mM) was chosen to achieve the same initial pH of approximately 11.3 as in the Na_2CO_3-based extraction while avoiding harsher alkaline conditions that could potentially increase the risk of uncontrolled chemical effects (e.g. more pronounced polymer hydrolysis/degradation). This approach allowed both extractions to start from equivalent pH conditions while maintaining consistency with the reference literature protocol for Na_2CO_3 [22]. Even in the absence of pH control strategies, the pH values at the end of the thermo-alkaline stage were recorded and reported as average value ± standard deviation among the extraction replicates carried out for each protocol.

For both NaOH- and Na_2CO_3-based extractions, the supernatant containing the solubilized EPS was collected after centrifugation (4000 · g, 4 °C, 20 min) and further processed via dialysis in demineralized water (SnakeSkin™ Dialysis Tubing, 3.5 kDa molecular weight cut-off MWCO, 35 mm, Thermo Scientific™; dialysis time ≈ 24 h with a liquid bulk replacement after approximately 12 ± 2 h). The aqueous dispersion thus obtained, referred to as EPS, was partially used for analysis and partly employed for the recovery of the hydrogel-forming EPS (the so-called structural EPS, sEPS). sEPS were extracted by acidic precipitation, by dosing 1 M HCl into the dialyzed EPS aqueous suspension up to pH = 2.20 ± 0.05 was achieved. To obtain homogeneous and stable sEPS aqueous suspensions, 1 M NaOH was progressively added to the acidic pellets of sEPS recovered after centrifugation (4000 · g, 4 °C, 20 min) up to pH = 8.5. This re-suspension stage influences the physicochemical and structural properties of sEPS, promoting the establishment of more extended polymer chain conformations with enhanced exposure of reactive functional groups. This structural arrangement is beneficial for the subsequent ionic cross-linking process, ultimately affecting the formation and stability of the hydrogel network. The main reason for using NaOH for both extractions was that NaOH, being a strong base with high solubility in water, allows pH regulation with the addition of a significantly lower volume of base solution, therefore minimizing the dilution of the sEPS extracts.

Referring to the thermo-alkaline stage, it is worth noting that, although the NaOH- and Na_2CO_3-based extractions were initiated at approximately the same pH, NaOH and Na_2CO_3 exhibit substantially different buffering capacities and intrinsic chemical properties, which could reasonably influence the extraction process. The experimental design was therefore conceived to reflect practical recovery scenarios, in which extraction agents were applied without active pH control. Consequently, the comparison presented in this study should be interpreted as descriptive of the overall extraction behavior under the tested conditions, rather than as a strictly controlled assessment of the intrinsic chemical effects of the reagents at identical buffering capacities or constant pH.

Total solids (TS) and volatile solids (VS) of AGS, EPS and sEPS were determined according to standard methods [37]. Concentrations of both EPS and sEPS aqueous suspensions were expressed as TS to WW mass ratios (i.e. wt% = g TS/g WW · 100 %) and the extraction yields were therefore calculated on a VS basis as mass ratio of extracted EPS/sEPS to initial AGS. Each extraction was carried out in triplicate and the results were hence expressed as average value ± standard deviation. EPS and sEPS aqueous suspensions obtained with both NaOH- and Na_2CO_3-based protocols were analyzed by a Varian 720-ES Inductively Coupled Plasma-Atomic Emission Spectrometer (ICP-AES) equipped with a pneumatic nebulizer to determine their concentrations of Ca, Cu, Fe, K, Mg, Mn, Na, Ni, P and Zn (expressed as mmol/g TS) and hence provide further information regarding the elemental composition of both EPS and sEPS resulting from the comparative extractions.

sEPS hydrogels of about 2 mm thickness and 26 mm diameter were formed via ionic cross-linking, by providing Ca^{2+} diffusion from an external aqueous solution into the polymeric matrix through a dialysis membrane. To this aim, sEPS aqueous suspensions at increasing sEPS concentrations (i.e. 0.6, 1.2 and 1.9 wt%) were placed into hollow

plastic supports having a disk-like geometry which were covered on the bottom through dialysis membrane sheets (SnakeSkin™ Dialysis Tubing, 3.5 kDa MWCO, 35 mm, Thermo Scientific™) and kept immersed into 2.5 % (*w/v*) $CaCl_2$ solutions for about 24 h [23,24].

2.2. Fractionation by size exclusion chromatography (SEC)

The sEPS samples (in the form of acidic pellets) from both NaOH- and Na_2CO_3-based extractions were solubilized in demineralized water to a concentration of 10 mg TS/mL, adjusting pH to 10 with NaOH. All solutions were centrifuged (3180 · g, 20 °C, 20 min) and then filtered through a 0.45 μm membrane filter before application to the column to ensure that the samples remained as dissolved as possible.

Size exclusion chromatography (SEC) was conducted by using a Hiload 16/600 Superose 6 prepacked column (Cytiva Lifesciences, Marlborough, MA) fitted on a Gilson system containing a UV (280 nm) detector, as described by Chen et al. [38]. Calibration of the column, upon which the elution volume was determined, was carried out through a Cytiva high-molecular weight marker set (Cytiva Lifesciences, Marlborough, MA). This consisted of ovalbumin (44 kDa), conalbumin (75 kDa), aldolase (158 kDa), ferritin (440 kDa), thyroglobulin (669 kDa) and blue dextran (2000 kDa). Blue dextran is typically included to evaluate the void volume, but Superose 6 has a very high fractionation range: fractionation range MW ~ 5–5000 kDa (globular proteins) and exclusion limit MW ~ 40,000 kDa (globular proteins); even blue dextran is retained in the column [38].

15 mL of solubilized sEPS samples were run through the column with a flow rate set to 1 mL/min, using a running buffer containing 0.15 M (NaCl) and 0.05 M (glycine) brought to pH 10 by adding NaOH. Three different fractions were selected based on the retention times of the different proteins in the high-molecular weight marker kit and the extrapolation of the calibration line. sEPS fractions were then dialyzed to remove excess salts through a 3.5 kDa MWCO dialysis bag (Snakeskin, ThermoFisher Scientific, Landsmeer), frozen at −80 °C and freeze-dried [38]. The freeze-dried samples thus obtained were stored at room temperature until use in further analysis.

The freeze-dried sEPS fractions from both NaOH- and Na_2CO_3-based extractions were characterized by Fourier transform infrared (FT-IR) spectroscopy to assess their main functional groups. FT-IR spectra were collected with a FTS-40 BioRad (USA) spectrometer (with a resolution of 4 cm^{-1} and 64 scans). The freeze-dried sEPS samples were homogeneously dispersed in a KBr pellet to collect their FT-IR spectra.

2.3. Determination of total protein and carbohydrate contents

Freeze-dried EPS, sEPS and sEPS fractions from SEC fractionation were dissolved in 0.01 M NaOH to 0.5 mg TS/mL prior to analyses. The total protein content was determined through the BCA protein assay according to the manufacturer's instruction by using bovine serum albumin (BSA) as a standard (Pierce BCA protein assay Kit, Thermo Scientific). Protein absorbance was measured in duplicates at 562 nm by employing a multimode plate reader (TECAN Infinite M200 PRO, Männedorf, Switzerland) [38]. The total carbohydrate content was determined, after diluting the EPS / sEPS / fractionated sEPS solutions 2.5 times, through the phenol sulfuric acid method by using glucose as a standard. The carbohydrate absorbance measurements were carried out in cuvettes at 490 nm in duplicates with a VIS-spectrophotometer (HACH DR3900, Ames, IA) [38]. Concentrations of proteins (PN) and carbohydrates (PS) in the samples were expressed as BSA and glucose equivalents, respectively.

2.4. Thermogravimetric (TG) and derivative thermogravimetric (DTG) analysis

Thermogravimetric (TG) and derivative thermogravimetric (DTG) analyses of freeze-dried EPS and sEPS samples from both NaOH- and Na_2CO_3-based extractions were carried out with a Q5000 TA Instruments thermogravimetric analyzer. The samples were heated from room temperature up to 600 °C at 10 °C/min under a nitrogen atmosphere (flow rate equal to 100 mL/min). The deconvolution of the DTG curves was performed by using the Multipeak fitting function of IGOR Pro software. The multiple Gaussian model that gave the highest R-square value was chosen to fit the experimental DTG curves [23].

2.5. Lipopolysaccharides (LPS) visualization using the polymyxin B-based fluorescent probe

Liposaccharides (LPS) were recently recognized as EPS components that could potentially contribute to the overall hydrogel-forming capacity of AGS-derived EPS [27]. In this regard, LPS were visualized through staining techniques in sEPS from both NaOH- and Na_2CO_3-based extractions to support the outcome of both rheology and SAXS measurements. LPS visualization was carried out by using the polymyxin B-based fluorescent probe, as reported by Li et al. [27]. Polymyxin B labelled with Rhodamine B was used to verify the presence of LPS and visualize their structure and morphology in the extracted sEPS. The mechanism of the staining is that polymyxin B interacts with LPS molecules via their cationic l-α-γ-diaminobutyric acid (Dab) side chains and the hydrophobic residues [27,39]. sEPS acidic precipitates were washed with 1xPBS twice and then incubated with polymyxin B labelled with Rhodamine B solution (1.1 μg/mL) at room temperature for approximately 2 min. The pellets collected after centrifugation were washed 4 times with 1xPBS to remove the residual probes. The samples were finally resuspended in 100 μL of 1xPBS to immediately collect fluorescence imaging. The images of polymyxin B with fluorescent probe Rhodamine B were captured with a CY3 filter [27].

2.6. Small-angle X-ray scattering (SAXS)

For both NaOH- and Na_2CO_3-based extractions, synchrotron small-angle X-ray scattering (SAXS) measurements were carried out on sEPS hydrogels formed at increasing sEPS concentrations (i.e. 0.6, 1.2 and 1.9 wt%) to investigate their network structure at nano-scale. The experiments were carried out at the ID02 beamline of the European Synchrotron Radiation Facility (ESRF, The European Synchrotron, 71 Avenue des Martyrs, CS40220, 38043 Grenoble Cedex 9) [40]. A scattering Q vector range of $0.003 \leq Q \leq 0.4$ $Å^{-1}$ was achieved using two sample–detector distances (1 m and 10 m) with a single-beam setup for monochromatic X-ray radiation at a 1 Å wavelength (12.46 keV). The beam size was 50 μm × 120 μm (vertical × horizontal) with a divergence of 5 μrad × 10 μrad. A 2 mm beamstop was used. The detector was a 2D Rayonix MX-170HS with a 44 × 44 $μm^2$ pixel size, positioned in an evacuated flight tube at either 1 m or 10 m from the sample. Exposure times were 0.5 s for the 1 m distance and 0.3 s for the 10 m distance. Scattering patterns were normalized to an absolute intensity scale after standard detector corrections and azimuthally averaged to obtain one-dimensional intensity profiles, I(Q) SAXS profiles were collected at 25 °C, in a solid sample-holder.

2.7. Rheology

For both NaOH- and Na_2CO_3-based extractions, the rheological features of sEPS hydrogels formed from sEPS suspensions with increasing sEPS concentrations (i.e. 0.6, 1.2 and 1.9 wt%) were assessed through frequency sweep measurements carried out with a Discovery Hybrid Rheometer (Disc.HR-3, TA Instruments) working in a controlled shear stress mode by using a plate-plate geometry (20 mm diameter, 400 μm gap). The trend of the storage modulus G' and loss modulus G'' as a function of the oscillation frequency was studied in the linear viscoelastic region (LVR) of deformations. The LVR was preliminarily determined for all tested samples through amplitude sweep measurements of G' and G'' performed at a constant frequency of 1 Hz by progressively

increasing the strain amplitude (Fig. S1). The normal force was set equal to 0.5 N in all measurements. All these experiments were carried out at a constant temperature of 25.00 ± 0.01 °C.

3. Results and discussion

3.1. Extraction performance

The extraction performance of the NaOH- and Na_2CO_3-based methods are compared in Table 1. The average EPS/sEPS extraction yields observed by using the Na_2CO_3-based extraction were in line with those reported in previous studies applying similar Na_2CO_3-based protocols [17,23]. Conversely, the average EPS and sEPS extraction yields decreased by about 67 % and 71 %, respectively, by using NaOH instead of Na_2CO_3 in the thermo-alkaline treatment (Table 1). In this regard, it should be considered that pH decreased down to values of approximately 6.89 ± 0.52 at the end of the thermo-alkaline stage in the NaOH-based extraction. Conversely, the use of Na_2CO_3 ensured more stable alkaline conditions during the biomass incubation period, resulting in a final pH of about 10.20 ± 0.24. The decrease in pH occurring during the EPS solubilization stage in the NaOH-based extraction could be reasonably ascribed to the progressive neutralization of the base by the biomass. This effect was much less pronounced when using Na_2CO_3 due to the well-known buffering capacity of carbonate. The increase in pH is reported to be effective in solubilizing the EPS matrix [29,41], thus potentially contributing to the higher recovery yield observed for the Na_2CO_3-based extraction. Since no pH control strategies were applied in the EPS solubilization phase, the differences observed in extraction performance may arise from the combined influence of both pH evolution during extraction and inherent chemical properties of NaOH and Na_2CO_3. Distinguishing these contributions would require dedicated experiments that are encouraged in future research. Particularly, setting equivalent and controlled pH conditions along the entire thermo-alkaline stage could help to get valuable insights on the effects exerted by the different reactivity and base strength of the reagents employed. While the final recovery yield related to sEPS was significantly lower for the NaOH-based extraction (66 ± 1 mg VS/g VS_{AGS} vs. 227 ± 26 mg VS/g VS_{AGS} for NaOH and Na_2CO_3, respectively), the sEPS to EPS mass ratio did not significantly vary between the tested protocols (42 ± 2 vs. 43 ± 4 % by using NaOH and Na_2CO_3, respectively). Further considerations can be made looking at the biochemical characterization of the extracted biopolymers in terms of concentrations of proteins (PN) and carbohydrates (PS) (Table 1). For both NaOH- and Na_2CO_3-based protocols, total EPS had significantly higher PN concentrations than sEPS. Consistently, the average PN to PS mass ratios (PN/PS) decreased in sEPS with respect to EPS indicating an increase in the relative content of PS: this evidence would suggest that acidic precipitation was more selective towards carbohydrates. It can be noticed that the average PN concentration in EPS from NaOH-based extraction was lower than that observed by using Na_2CO_3; a reduction in the PN concentration was also detected for sEPS by applying the NaOH-based protocol. While polysaccharides are generally relatively more stable to alkali, proteins are reported to be sensitive to degradation under alkaline conditions [29]. The extent of PN degradation may be even higher by using a strong base as NaOH coupled with high temperatures that could induce, above certain threshold conditions, hydrolysis of peptide bonds and reduction of polypeptide size [29,42]. In line with these observations, the average PN to PS mass ratios observed for the NaOH-based extraction were lower than those measured for the Na_2CO_3-based method, with a more pronounced difference in EPS than in sEPS. In this regard, different PN and PS recovery efficiencies via acidic precipitation could be predicted for the tested extraction protocols, especially regarding carbohydrates. Referring to the average PN and PS concentrations listed in Table 1, it was inferred that the acidic precipitation allowed to recover approximately 28 and 33 wt% of PN and PS, respectively, from solubilized EPS in the NaOH-based protocol. Conversely, the acidic stage in the Na_2CO_3-based extraction led to higher recovery efficiencies of PN and PS from solubilized EPS – accounting for about 34 and 50 wt%, respectively – thus evidencing a higher effectiveness especially in precipitating carbohydrates. These results therefore suggested that the extraction conditions applied in the alkaline stage may influence the precipitation ability of the distinct polymeric classes under acidic conditions. Denaturation, degradation and/or structural alterations of polymers – resulting in changes in molecular weight distribution and/or spatial conformation – may occur depending on the alkaline solubilization conditions applied, thus affecting the efficiency of the final (acidic) recovery stage [29]. NaOH, due to its strong base nature and higher reactivity, is expected to exert harsher effects on characteristics, such as molecular weight, chain conformation and intermolecular interactions, of certain EPS fractions, thus potentially reducing the efficiency of their subsequent recovery via acidic precipitation [29]. For instance, the higher protein hydrolysis likely promoted by NaOH would reduce the molecular weight of protein-carbohydrate complexes, thus reasonably decreasing their precipitation yield. In contrast, Na_2CO_3, thanks to its milder chemical effects, could help to preserve the integrity of protein-carbohydrate complexes, with positive implications for their recoverability during the acidic stage, thus ultimately contributing to an increase in the PS precipitation efficiency.

Experimental findings from the literature reveal a lack of consensus on the extraction effectiveness of NaOH- and Na_2CO_3-based protocols [29,36]. Bou-Sarkis et al. [29] observed that the use of NaOH instead of Na_2CO_3 can more efficiently solubilize the EPS matrix of AGS, while decreasing the final yield of gel-forming EPS (i.e. sEPS). Conversely, Le et al. [36] reported higher recovery yields of sEPS from activated sludge by applying NaOH-based extractions rather than similar methods using Na_2CO_3. In this regard, it should be considered that even minor differences in terms of operative conditions applied (e.g. pH, reagent dosage, etc.) could significantly affect the extent and characteristics of recoverable EPS. For instance, in contrast with the present study, both Bou-Sarkis et al. [29] and Le et al. [36] carried out comparative thermo-alkaline extractions under different initial pH conditions (about 13.40 / 13.01 for NaOH and 11.30 / 10.01 for Na_2CO_3, respectively): in these previous works, the higher pH associated with the NaOH-based protocols could have contributed to increase their extraction performance in the alkaline stage. Moreover, it should be noted that the use of a strong base as NaOH, combined with high pH conditions, could enhance cell lysis processes [36], with implications for the estimation of recovery yields.

When NaOH was used as alkaline solubilization agent, the resulting sEPS (acidic) pellets qualitatively appeared more loosely structured than those obtained from the Na_2CO_3-based extraction. Following centrifugation, the lower apparent cohesion of the sEPS precipitates hindered efficient solid-liquid separation, thus hampering the pellet recovery from supernatant. Consequently, the sEPS obtained from the NaOH-

Table 1
Extraction yields and total protein (PN) and carbohydrate (PS) contents of EPS and sEPS recovered by both NaOH- and Na_2CO_3-based extractions. Extraction yields are reported on a VS basis as average value ± standard deviation among n. 3 extractions carried out for each protocol. Concentrations of PN and PS are expressed as BSA and glucose equivalents, respectively.

	NaOH		Na_2CO_3	
	EPS	sEPS	EPS	sEPS
Extraction yield (mg VS/g VS_{AGS})	165 ± 14	66 ± 1	499 ± 58	227 ± 26
VS/TS (mg VS/g TS)	909 ± 29	886 ± 64	843 ± 7	883 ± 13
PN (mg/g VS)	475 ± 10	328 ± 8	522 ± 9	392 ± 5
PS (mg/g VS)	245 ± 9	205 ± 11	204 ± 3	226 ± 10
Average PN/PS (g/g)	1.94	1.60	2.56	1.73

based extraction could not be concentrated above about 1.9 wt% by centrifugation (even applying consecutive centrifuges, as described by Pagliaccia et al. [17]), while significantly higher sEPS concentrations were achieved when Na_2CO_3 was used as alkaline extraction agent. Although this evidence regarding the cohesion of acidic pellets resulted only from qualitative observations rather than dedicated quantitative measurements, it was reproducible across independent extraction replicates and systematically noted during sample handling. Furthermore, this observation was in line with differences in the sEPS composition and structural arrangement inferred from subsequent analyses. A potential reason could be found in the more intensive hydrolysis/degradation of certain EPS fractions (e.g. proteins) reasonably caused by NaOH [29], likely resulting in the partial loss of their tertiary structure and in a reduction in their molecular weight, as reported in the following section regarding SEC fractionation. Moreover, it should be pointed out that the molar ratio of divalent to monovalent ions in sEPS, calculated based on the predominant valence of the elements measured by ICP-AES (Table S1), was significantly higher for the extractions using NaOH instead of Na_2CO_3 in the thermo-alkaline stage (i.e. about 0.92 vs. 0.10 mol M^{2+}/mol M^{+}). As detailed in Section 3.5, this may have more readily contributed to a partial (albeit limited) cross-linking of NaOH-extracted sEPS even in the absence of exogenous Ca^{2+}, thus potentially hindering dehydration by centrifugation.

3.2. Molecular weight-based fractionation of sEPS by size exclusion chromatography (SEC)

SEC fractionation of freeze-dried sEPS revealed different molecular weight (MW) profiles depending on the extraction conditions applied, as detailed in Table 2. For both NaOH- and Na_2CO_3-based protocols, the relative abundance of the different MW-based fractions decreased in the following order: F3 (3.5–100 kDa) > F1 (738–5500 kDa) > F2 (100–738 kDa) (with mass percentages of F1 only slightly higher than F2 for Na_2CO_3). The abundance of polymeric fractions between 3.5 and 100 kDa was already reported by Chen et al. [38] for EPS from both aerobic and anaerobic granular sludge. Overall, the use of a Na_2CO_3-based alkaline stage resulted in a higher relative content of MW-based fractions >100 kDa in the fractionated sEPS (F1 + F2 ≈ 55 vs. 40 % on a mass basis for Na_2CO_3- and NaOH-based extractions, respectively; Table 2). The lower mass percentage of high-molecular weight constituents recovered via SEC fractionation for the NaOH-based protocol is consistent with literature data. As previously discussed, the combination of a strong base such as NaOH and high temperatures (e.g. 80 °C) can significantly alter the macromolecular structure and integrity of some EPS compounds. These harsh conditions could reasonably promote hydrolysis/partial degradation of high-MW biopolymers (e.g. large proteins), leading to a more pronounced shift in the molecular weight distribution towards smaller molecules. This size reduction effect was also documented by Bou-Sarkis et al. [29] for sEPS extracted from AGS through a NaOH-based protocol. It is worth noting that the mass percentage of the non-soluble fraction was higher for the NaOH-based extraction (18 vs. 10 % for NaOH- and Na_2CO_3-based protocols, respectively). The non-soluble fraction excluded from SEC fractionation is expected to contain a heterogeneous ensemble of macromolecular structures, reasonably including slightly cross-linked aggregates, insoluble carbohydrate-protein complexes and other recalcitrant macromolecular assemblies. In line with that described in the previous section, the higher M^{2+} concentrations of sEPS resulting from the NaOH-based protocol (Table S1) could support the hypothesis that a partial, albeit limited, polymer chain cross-linking may occur without dosing exogeneous divalent metal cations, hence potentially hindering polymer solubilization. Furthermore, NaOH-induced hydrolysis can break down certain molecular structures and favour the release of insoluble components, thus possibly increasing the overall mass fraction of non-soluble sEPS.

For the fractionated sEPS samples, PN and PS were detected in each MW fraction with variable concentrations (Table 2). For both NaOH- and Na_2CO_3-based extractions, the PN to PS ratio decreased as MW increased, as evidenced by Chen et al. [38]. The highest PN concentrations were found in F3 (437 ± 5 and 465 ± 5 mg/g VS in the cases of NaOH and Na_2CO_3, respectively, as BSA equivalents), hence associated with the lower MW constituents, while PS were more abundant in the high-MW fraction F1 (292 ± 5 and 256 ± 5 mg/g VS for NaOH and Na_2CO_3, respectively, as glucose equivalents). For each MW-based fraction, fractionated sEPS obtained via the Na_2CO_3-based protocol had higher PN to PS ratios compared to those observed for the NaOH-based extraction (1.37–2.20 vs. 1.10–1.92 g/g), in line with that evidenced above for non-fractionated sEPS (Table 1).

Regardless of the EPS recovery approach applied, FT-IR spectra of the distinct MW-based fractions of sEPS (Fig. S2) revealed the main functional groups related to proteins and polysaccharides, in line with literature data on AGS-derived sEPS [18,23]. For more details on peak assignment refer to Table S2. FT-IR analysis showed similar spectral features for both NaOH- and Na_2CO_3-based extractions. Similarly, Le et al. [36] found that the FT-IR spectra of EPS extracted from activated sludge through NaOH- and Na_2CO_3-based thermo-alkaline treatments exhibited similar functional groups. The above hence suggested that the core biochemical signature of sEPS fractions would be mostly maintained regardless of the (alkaline) extraction conditions applied.

3.3. Thermogravimetric (TG) and derivative thermogravimetric (DTG) analysis

For both EPS and sEPS obtained by NaOH- and Na_2CO_3-based extractions, thermograms from TG and DTG analysis recorded between 25 and 600 °C (Fig. S3) revealed two main stages of thermal decomposition: (i) evaporation of residual moisture up to about 132–150 °C (i.e. dehydration leading up to 11 wt% weight loss), and (ii) pyrolysis of organic matter, in the temperature range between approximately 150 and 550 °C [23,43]. Decomposition of minerals present in EPS/sEPS was not significantly appreciated in the TGA and DTG curves, since it usually occurs at higher temperatures (typically in the range of about 600 °C to 800 °C [43]). It is worth noting that the thermal degradation of organics of both EPS and sEPS from Na_2CO_3-based extraction started at slightly

Table 2
Fractionation yields by size exclusion chromatography (SEC) of sEPS (after freeze-drying) from NaOH- and Na_2CO_3-based extractions and characterization of each molecular weight (MW)-based fraction in terms of total protein (PN) and carbohydrate (PS) contents. Fractionation yields are reported as percentage on a mass basis of fractionated sEPS. Concentrations of PN and PS are expressed as BSA and glucose equivalents, respectively.

		Fractionation yield (%)		PN (mg/g VS)		PS (mg/g VS)		Average PN/PS (g/g)	
Fraction (#)	MW (kDa)	NaOH	Na_2CO_3	NaOH	Na_2CO_3	NaOH	Na_2CO_3	NaOH	Na_2CO_3
1	738–5500	22	28	320 ± 8	350 ± 4	292 ± 5	256 ± 5	1.10	1.37
2	100–738	18	27	298 ± 10	352 ± 9	263 ± 2	228 ± 4	1.13	1.54
3	3.5–100	42	35	437 ± 5	465 ± 5	228 ± 8	211 ± 7	1.92	2.20
Non-soluble [a]		18	10						

[a] The non-soluble fraction was not part of the SEC-based fractionated samples, as also reported by Chen et al. [38].

higher temperatures than those observed for samples obtained through the NaOH-based protocol (149 and 137 °C for EPS and sEPS, respectively, by using Na_2CO_3, vs. about 132 °C for both EPS and sEPS from NaOH-based extraction). This evidence would suggest that the Na_2CO_3-based protocol may have enabled the extraction of more complex macromolecules that reasonably required higher energy to be thermally decomposed.

Further insights into the thermal behavior of EPS/sEPS were gathered from the deconvolution of the DTG curves in the temperature range from 125 to 500 °C (Fig. 1). Regarding total EPS, deconvolution of DTG signals revealed the presence of four partially overlapping thermal events, which can be associated with distinct pyrolytic processes. However, these events were not fully resolved from each other, indicating a partial simultaneity in the degradation of different EPS components. Although a precise deconvolution into four discrete chemical species was not feasible based solely on the observed thermal transitions, hypothesis on the EPS fractions contributing to the recorded DTG signals can be made thanks to the comparison with previous scientific reports. Particularly, for increasing temperatures, contributions from low thermal resistant proteins (PNI), PS and high thermal resistant proteins (PNII), respectively, could be reasonably predicted in agreement with literature data [23]. In the case of sEPS, deconvolution of the DTG curves revealed two predominant thermal events. Similar to total EPS, these thermal events were partially overlapping, again suggesting the partial simultaneity in the observed pyrolytic processes. The first event, exhibiting a peak at approximately 280 °C for both NaOH- and Na_2CO_3-based extractions, could be reasonably attributed to the degradation of PS. This assignment is consistent with literature data, according to which the thermal decomposition of carbohydrates typically occurs in the temperature range from 220 to 300 °C [23,36,43]. A broader DTG signal was associated with the second thermal event, with a peak centered at around 311 and 344 °C for NaOH- and Na_2CO_3-based protocols, respectively. This process covered a wider temperature domain and could be reasonably ascribed to the pyrolytic breakdown of high-molecular weight fractions, potentially including proteins with complex tertiary structures and/or glycosylated proteins, that are expected to have greater thermal stability. Glycoproteins, whose presence in EPS was documented in the literature [7], are indeed reported to have peak degradation temperatures in the range between 320 °C and 350 °C [44,45]. According to literature evidence, potential contributions to the DTG signals in this temperature domain could also arise from lipids [46], phospholipids [47] and lipopolysaccharides [48].

When interpreting thermograms, it should be considered that all chemical assignments here suggested for the deconvoluted DTG curves are purely speculative since no complementary analytical techniques were employed for validation. DTG deconvolution was indeed intended to provide a qualitative interpretation of the observed thermal profiles rather than a definitive identification of individual EPS/sEPS components.

It is worth noting that, for both EPS and sEPS, most of the detected pyrolytic events exhibited a shift towards higher temperature domains when the Na_2CO_3-based protocol was employed (Table S3), thus potentially indicating the extraction of more thermally resistant polymers. This evidence was consistent with the results from SEC fractionation (Table 2), revealing that the Na_2CO_3-based protocol enabled the recovery of larger quantities of high-molecular weight fractions: these larger macromolecules are expected to have more complex structures, therefore requiring increased thermal energy for thermal degradation.

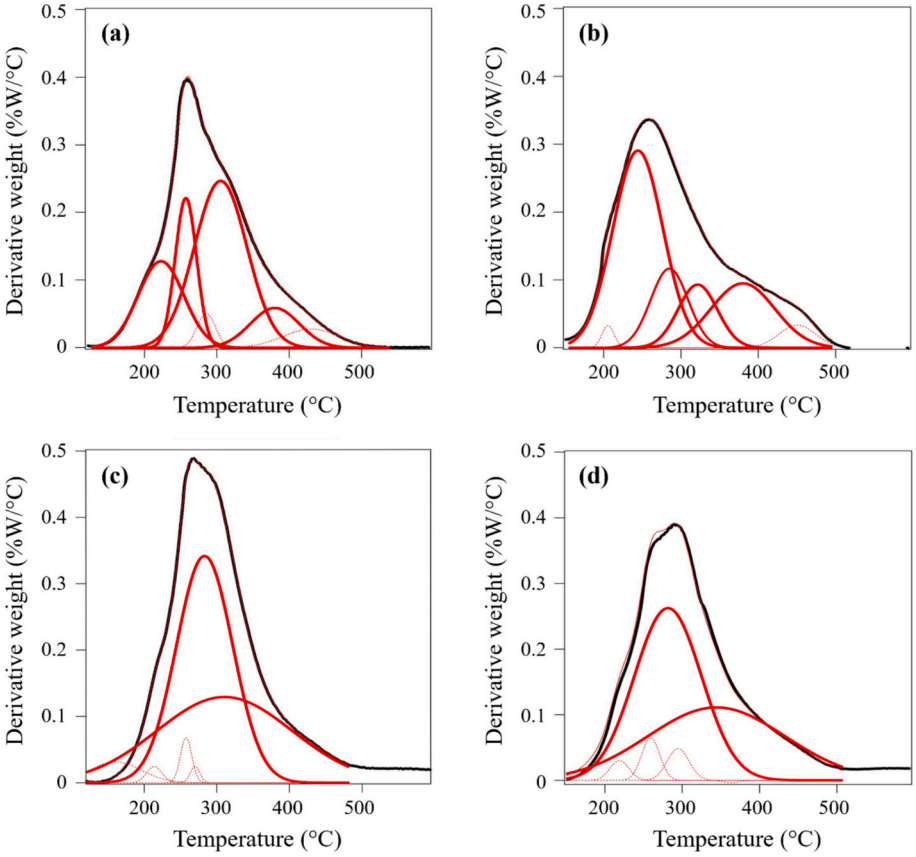

Fig. 1. Derivative thermogravimetric (DTG) curves (black lines) and corresponding deconvoluted signals (red lines) for EPS / sEPS from NaOH-based extraction (a / c) and for EPS / sEPS from Na_2CO_3-based extraction (b / d). The red solid / dashed lines refer to the Gaussian contributions whose area is higher / lower than 5 % of the total area subtended by the DTG curve, respectively. The latter (dashed lines) are therefore marginal contributions that were not considered in the discussion.

3.4. Structural insights on sEPS hydrogels through small-angle X-ray scattering (SAXS) measurements

SAXS measurements enabled structural investigation of sEPS hydrogels across multiple length scales – from the molecular level, captured at high scattering vector (Q) values, to the larger-scale network architecture, revealed at low Q [49]. To capture these distinct structural features, SAXS profiles of sEPS hydrogels at different sEPS concentrations were recorded over a wide Q range (Figs. 2a and b for NaOH- and Na_2CO_3-based extractions, respectively), and their low-Q and high-Q regions were analyzed separately (Figs. 2c and d, respectively).

Fig. 2c displays SAXS profiles of sEPS hydrogels at different sEPS concentrations (log-log scale plots) restricted to the low-Q region (0.0035–0.06 $Å^{-1}$). In this regime, scattering intensities of sEPS hydrogels from NaOH-based extraction lacked a plateau at lowest Q values, indicating the absence of a Guinier region [50]. This would indicate that the characteristic size of hydrogel structural components was larger than the captured Q-range, i.e. $> 2\pi/Q_{min} = 180$ nm (where Q_{min} is the lowest recorded scattering vector), meaning that the scattering radiation primarily probes the local network structure. In this low-Q regime, the scattering intensity followed a power law behavior, $I(Q) \propto Q^{-n}$, where the exponent n is graphically given by the slope of the log-log plot in Fig. 2c. For hydrogel systems, n typically represents the fractal dimension, reflecting the degree of self-similarity within the hydrogel network and describing how mass scales with volume [50]. Fitting the experimental data with this model yielded a fractal dimension of $n \approx 2.6$ for all sEPS concentrations (Table S4), indicating that the hydrogel network was likely composed of three-dimensional mass fractals with intermediate compactness, which remained almost invariant with respect to the sEPS concentration [51]. For more details on the model fitting refer to Section S1 in *Supplementary material*. Fractal dimensions in this range are associated with heterogeneous, space-spanning networks in which the polymer mass is distributed in a non-uniform manner, reflecting a relatively high degree of compactness typical of physically cross-linked hydrogel systems [52].

In contrast, SAXS profiles of sEPS hydrogels from Na_2CO_3-based extraction displayed a two-power law behavior, visible by the presence of two nearly linear regions in the log-log plots with different slopes, occurring across different Q-intervals. These profiles were fitted according to a two-power law empirical model (Section S1 in *Supplementary material*), yielding sEPS concentration-independent n values of approximately 2.8–2.9 in the 0.018–0.035 $Å^{-1}$ Q range and about 2 in the 0.0035–0.015 $Å^{-1}$ Q range (Table S4). Consistent with the analysis of sEPS hydrogels from NaOH-based extraction, the n value in the 0.018–0.035 $Å^{-1}$ Q range indicated the presence of three-dimensional mass fractals, with slightly higher compactness than those observed

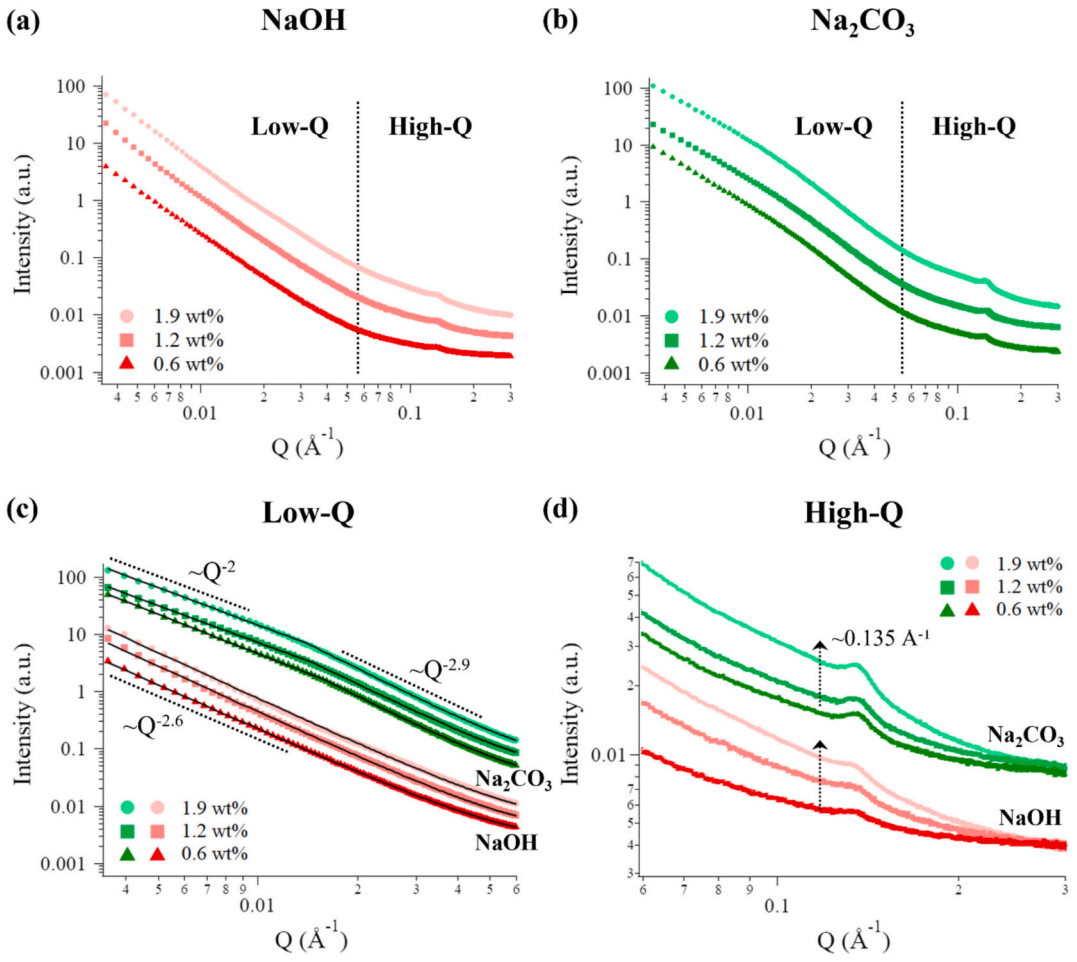

Fig. 2. SAXS profiles (log-log scale plot) of sEPS hydrogels from both NaOH-based extraction (a) and Na_2CO_3-based extraction (b) for increasing sEPS concentrations, together with the corresponding profile analysis performed in the low-Q (c) and high-Q (d) regions. In panel (c), the experimental profiles (data shown as symbols) are reported together with the corresponding best-fit curves (solid black lines), obtained using a single power law empirical model for sEPS hydrogels from NaOH-based extraction and a two-power law empirical model for sEPS hydrogels from Na_2CO_3-based extraction (see Section S1 in *Supplementary Material*). The slopes of the linear regions in the log-log plots extracted from the fits are indicated by dotted black lines, along with the corresponding power law exponents. In panel (d), black arrows indicate the *Bragg peak* of the sEPS hydrogels, whose intensity increases with increasing sEPS concentrations for both NaOH- and Na_2CO_3-based extractions. The Q value corresponding to the *Bragg peak* maximum is also reported in the figure. In all panels, SAXS profiles are offset for the sake of clarity.

for the NaOH-based protocol. However, the emergence of an additional power law behavior at lower Q values suggested the coexistence of this fractal network with an additional structural motif, which was not observed in sEPS hydrogels from NaOH-based extraction. Specifically, the $I(Q) \propto Q^{-2}$ functional behavior can be associated with scattering from two-dimensional structures with a lamellar shape [51]. Interestingly, a similar lamellar, multilayered morphology was recently reported for LPS-Ca aggregates from AGS-derived EPS and positively linked to the formation of self-standing sEPS hydrogels [27]. This aggregation pattern was attributed to the unique molecular composition of LPS in aerobic granular sludge, where the hydrophobic and hydrophilic components of LPS (lipid A and glycans, respectively) have comparable effective molecular cross-sectional areas, favoring a lamellar packing [27]. Based on these findings, it is reasonable to hypothesize that similar lamellar structures – likely associated with LPS assemblies – could be present in the sEPS hydrogels from Na_2CO_3-based extraction.

To complete the morphological and size-related analysis, the investigation also involved the high-Q region (0.06–0.30 $Å^{-1}$) of the SAXS profiles (Fig. 2d), which encodes smaller, molecular-scale structural information. In this regime, SAXS profiles of sEPS hydrogels from both NaOH- and Na_2CO_3-based protocols displayed a diffraction correlation peak, commonly referred to as a *Bragg peak*, indicating the presence of a highly ordered, periodic arrangement. The corresponding characteristic spacing can be calculated using Bragg's law: $d = 2\pi/Q_{max}$, where Q_{max} is the position of the peak maximum [50]. Q_{max} values for different sEPS hydrogels were located at approximately 0.135 $Å^{-1}$, revealing a consistent d-spacing of about 47 Å across all samples. Surprisingly, the d-spacing observed in this study closely matches values previously reported for EPS hydrogels from anammox granular sludge [9]. This scattering feature here detected would suggest the presence of well-defined structural motifs with a characteristic periodic spacing. Notably, this *Bragg peak* feature would be consistent with the lamellar, multilayered LPS structures inferred from the low-Q SAXS profiles of sEPS hydrogels from Na_2CO_3-based protocol and previously observed by Li et al. [27] in LPS-Ca aggregates from AGS-derived EPS. In this context, the observed d-spacing likely corresponded to the center-to-center distance between adjacent LPS bilayer stacks arranged in a layered configuration. A similar *Bragg peak* was also observed in SAXS profiles of other polysaccharide gels, where it was ascribed to the presence of ordered bilayer-like structures interconnecting polymer chains into a three-dimensional network [53], thus further supporting the proposed data interpretation.

In sEPS hydrogels from Na_2CO_3-based extraction the intensity of the *Bragg peak* increased with rising sEPS concentration, while its position remained unchanged. This suggested that higher sEPS concentrations led to an increased presence of lamellar multilayered structures within the hydrogel, likely due to a corresponding enrichment in the LPS component responsible for their formation. Interestingly, a *Bragg peak* was also observed in sEPS hydrogels from NaOH-based extraction (at the same Q value) despite the absence of lamellar-related features in the low-Q region. However, the peak exhibited a significantly lower intensity, suggesting that, while multilayered structures can still be present, their concentration would likely be much lower. Hypothesizing that these lamellar, multilayered domains were largely associated with LPS assemblies, the lower degree of ordering in sEPS hydrogels from NaOH-based extraction might be due to a lower concentration of LPS components within the cross-linked matrix, or, alternatively, to a different chemical composition profile of LPS recovered with the two protocols, leading to diverse molecular packing and final structure. For instance, NaOH, being a strong base, could induce reactions similar to saponification, such as alkaline hydrolysis of ester bonds of lipidic portion of LPS, thus potentially leading to hydrolysis-like processes of LPS themself.

In this regard, further insights were obtained from the analyses aimed at visualizing LPS in sEPS by using the polymyxin B-based fluorescent probe (Fig. 3). Polymyxin B specifically binds to the lipid A in LPS. By labelling with Rhodamine B as the fluorescence probe, the presence and specific morphologies of LPS can be clearly visualized with the fluorescence signal [27]. Significant differences were observed in sEPS depending on the applied recovery approach. Only weak fluorescence signals were observed from the sEPS extracted with the NaOH-based protocol, meaning that they had a relatively low content of LPS. Contrarily, sEPS obtained through the Na_2CO_3-based extraction exhibited a strong fluorescence signal, suggesting the presence of bilaminar multilayered structures (*onion-like*) and an overall higher abundance of LPS assemblies. This evidence hence corroborated the hypothesis inferred from SAXS analysis. The use of complementary techniques such as cryogenic electron microscopy (cryo-EM) and/or small-angle neutron scattering (SANS) is encouraged in future studies to provide additional support for the structural arrangements deducted from the SAXS-based interpretation. Notably, SANS could offer further insights through contrast variation, enabling a more selective assessment of LPS-rich assemblies within the complex EPS matrix.

3.5. Rheology of sEPS hydrogels

Fig. 4 shows the frequency sweep curves obtained in the LVR for sEPS hydrogels formed from sEPS suspensions at 0.6, 1.2 and 1.9 wt% sEPS concentrations. For both NaOH- and Na_2CO_3-based extractions, the storage modulus G' and loss modulus G'' did not considerably vary with increasing frequency in the log-log scale plot visualization. As observed in previous studies [23,24], for all sEPS concentrations investigated, G' was higher than G'' in the applied ranges of frequencies while no crossover between G' and G'' profiles was detected. This rheological evidence suggested that all tested sEPS-based systems exhibited a solid-like behavior, thus being classified as gels from a rheological standpoint [54].

While hydrogels exhibiting solid-like mechanical responses across the entire range of sEPS concentrations explored, their G' (and G'') values significantly varied depending on the sEPS concentration. At a frequency of 1 Hz, G' increased up to 318 and 1373 Pa for Na_2CO_3- and NaOH-based extractions, respectively, by increasing the sEPS concentration to 1.9 wt% (Fig. 5). Such an increase in G' as sEPS concentration rises is well-documented in the literature [23,24] and can be mainly ascribed to a progressive increase in cross-linking density. Even if based on a limited interval of sEPS concentrations, the conclusions drawn from the observed mechanical profiles can be considered robust and reliable under the hydrogel-forming conditions here tested. The trends identified are indeed supported by consistent rheological evidence in agreement with literature data [23,24]. However, the above interpretations should be considered strictly valid only within the interval of sEPS concentrations here studied and cannot be directly extrapolated to significantly different conditions for which rheological data are not available. It should be noticed that the choice to investigate such a restricted spectrum of sEPS concentrations was guided by practical constraints. The lower limit (i.e. 0.6 wt%) was slightly above the minimum concentration required for hydrogel-formation in comparable sEPS-based systems [17]. The upper limit (i.e. 1.9 wt%) was instead imposed by the NaOH-based extraction, which yielded a maximum sEPS concentration of about 1.9 wt%, as detailed in Section 3.1.

For all tested concentrations, sEPS from NaOH-based extraction formed stiffer hydrogels compared to those obtained by using Na_2CO_3 in the EPS alkaline solubilization stage (Figs. 4 and 5). Many considerations could be made to explain this experimental evidence.

As highlighted above, sEPS extracted through NaOH- and Na_2CO_3-based protocols exhibited different concentrations of divalent metal ions M^{2+} (Table S1), resulting in M^{2+}/M^{+} molar ratios of approximately 0.92 vs. 0.10 mol M^{2+}/mol M^{+}, respectively. Since the hydrogel-formation of AGS-derived sEPS relies on M^{2+}-mediated ionic cross-linking mechanisms, these differences could partly contribute to the distinct rheological profiles observed for the comparative extractions. M^{2+} intrinsically

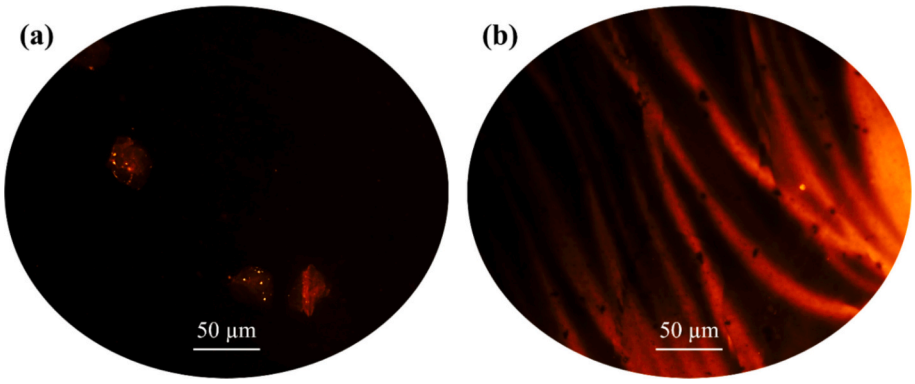

Fig. 3. Visualization of lipopolysaccharides (LPS) in sEPS extracted through the protocols employing NaOH (a) and Na_2CO_3 (b) in the thermo-alkaline stage by using polymyxin B labelled with Rhodamine B staining.

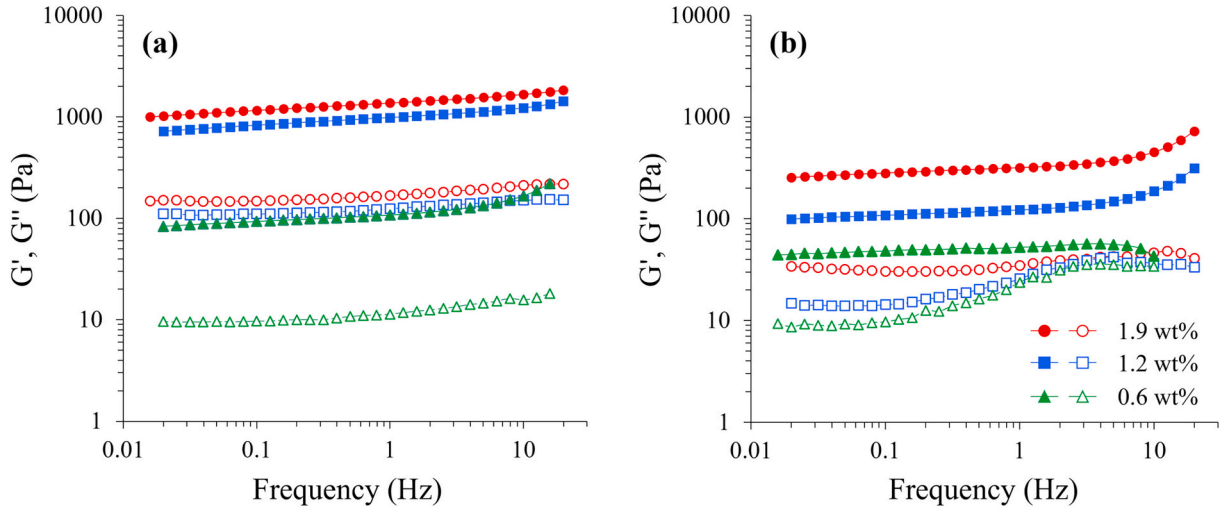

Fig. 4. Trend of storage modulus G' and loss modulus G'' of sEPS hydrogels at different sEPS concentrations as a function of oscillation frequency for both NaOH-based extraction (a) and Na_2CO_3-based extraction (b). G' and G'' values are reported as filled and open symbols, respectively. Both X- and Y-axes are shown on a logarithmic scale.

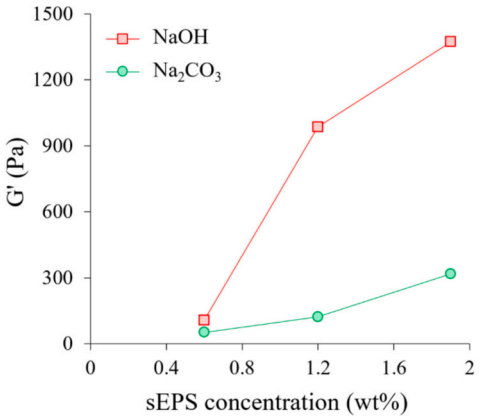

Fig. 5. Trend of storage modulus G' of sEPS hydrogels as a function of sEPS concentration for both NaOH- and Na_2CO_3-based extractions. G' values were obtained from the frequency sweep curves in Fig. 4 for a frequency of 1 Hz.

associated with the sEPS extracts could reasonably induce partial cross-linking, thus potentially affecting the final hydrogel mechanical response. However, this contribution is expected to be secondary compared to that arising from the exogenous Ca^{2+} intentionally added during hydrogel-formation. Indeed, the diffusion of Ca^{2+} ions into the polymeric matrix during ionic cross-linking typically leads to Ca^{2+} concentrations in the hydrogels significantly higher than those originally present in the pristine sEPS [17,23]. As documented in the literature, in the case of ionically cross-linked sEPS hydrogels, the storage modulus G' – directly correlated to the cross-linking density [55] – typically increases as Ca^{2+} concentration increases (at least up to a threshold concentration) [21]. Consequently, the overall mechanical behavior of sEPS hydrogels is expected to be primarily governed by the cross-linking induced by exogenous Ca^{2+}, while only a marginal contribution would be driven by M^{2+} originally present in the pristine sEPS. Referring to the NaOH-based protocol, it is therefore reasonable to suppose that the higher M^{2+} concentrations in the extracted sEPS (Table S1) may marginally contribute to the increased G' values observed for the resulting hydrogels, by providing an additional, albeit limited, cross-linking density to that induced by exogenously added Ca^{2+}.

Further research hypothesis may be proposed to explain the revealed rheological differences. Polysaccharides are known to be key EPS components involved in the hydrogel-formation [56]. In this regard, it should be noted that the NaOH-based protocol yielded slightly higher relative contents of carbohydrates in the extracted sEPS and related molecular weight-based fractions, as suggested by the average PN to PS ratios listed in Tables 1 and 2. One of the potential reasons for the lower G' values observed for sEPS hydrogels from the Na_2CO_3-based extraction

could be therefore associated with the presence of relatively large macromolecules (e.g. proteins) interpenetrated within the 3D polymeric network of the hydrogel without significantly contributing to its cross-linking density and strength. Large proteins could hence potentially interfere with the polysaccharidic 3D network by reducing the overall elastic response of the hydrogel. Thus, the harsher hydrolysis of the proteinaceous fraction likely induced by NaOH could contribute to increase the mechanical properties of cross-linked sEPS. This mechanistic hypothesis would be supported by both SEC fractionation (Table 2) and TGA-DTG analysis (Fig. 1) that suggested the higher abundance of large macromolecules (> 100 kDa) and high thermal resistant compounds in sEPS extracted through the Na_2CO_3-based protocol. SAXS measurements could also provide another potential explanation for the different rheological features observed. These analyses suggested that sEPS hydrogels were characterized by the presence of 2D objects (such as lamellae) arranged into multilayered assemblies (Fig. 2): such a structural motif resulted more abundant in the case of Na_2CO_3-based extraction and it was consistent with previous findings by Li et al. [27]. These characteristic structures, potentially associated with LPS assemblies, would contribute to the establishment of more ordered 3D networks, but could also make hydrogels mechanically weaker, as the lamellae could tend to align along the direction of the applied shear stress. In line with this interpretation, previous literature on surfactant-based systems has shown that 2D lamellar structures exhibit lower G' values than other supramolecular assemblies [57].

In summary, for both recovery approaches applied, AGS-derived sEPS formed self-standing hydrogels with solid-like mechanical properties. The rheological differences here highlighted in terms of hydrogel stiffness (G' values) between the NaOH- and Na_2CO_3-based protocols could be hence actually ascribed to modifications induced in the sEPS chemical, physicochemical and structural features by the overall extraction chemistry. In this regard, the use of a strong base such as NaOH may be reasonably associated with more intensive hydrolysis-like processes of specific components, such as proteinaceous and lipidic fractions, thus exerting a sort of selective "purification" of the sEPS extracts. These phenomena may have helped to reduce the presence of macromolecules and supramolecular arrangements that potentially do not contribute to, or even interfere with, the post-gelling mechanical strength (e.g. proteinaceous portion of glycoproteins, large proteins and LPS lamellar assemblies). Overall, these factors may have contributed to an increased hydrogel stiffness for the NaOH-based extraction.

While the above explanations regarding the hydrogel rheological differences observed for the NaOH- and Na_2CO_3-based extractions remain largely speculative, they are supported by the overall consistency of results obtained from the different methodologies applied. However, dedicated studies will be essential to validate the proposed mechanistic hypotheses. Future research could explore the role of macromolecule interpenetration within the cross-linked network by subjecting extracted sEPS to selective enzymatic treatments prior to hydrogel-formation. In line with experimental approaches already successfully applied [55], the targeted and controlled degradation of specific sEPS constituents, followed by the preparation and mechanical testing of single-fraction hydrogel-like systems, may help to elucidate the relative contribution of different polymeric classes to the overall rheological behavior. This methodological strategy would also provide insights into the neutral or potentially detrimental effect of non-gelling compounds on the sEPS hydrogel mechanics. Furthermore, coupling selective enzymatic treatments with MW-based fractionation could offer additional information on the combined influence of MW distribution and macromolecular identity on the viscoelastic response of sEPS hydrogels. Finally, the selective isolation of the LPS fraction from sEPS, followed by rheological and SAXS-related structural characterization of both LPS-depleted sEPS hydrogels and isolated LPS-derived cross-linked systems, would help to understand the influence of LPS assemblies on the mechanical properties of sEPS hydrogels.

Considerations on the gelling mechanisms could be typically inferred from rheological data. Based on the observed rheological profiles, previous works suggested a percolation model [58,59] to describe the hydrogel-formation of AGS-derived sEPS [23,24]. This model assumes a critical phenomenon of connectivity, according to which the formation of an "infinite" cross-linked 3D network occurs when the fraction of connected objects is above the so-called percolation threshold [60]. According to this percolative mechanism, in the formation of sEPS hydrogels, clusters composed of sEPS would be first established, followed by their progressive interconnection, ultimately giving rise to an "infinite" 3D network extended to the whole sample volume [23]. The gelation thresholds of AGS-derived sEPS were expressed in previous studies through conceptual phase diagrams in terms of minimum M^{2+} concentration in the cross-linker solution and minimum sEPS concentration that allow to form hydrogels [17,24]. In this work, all tested sEPS concentrations enabled the formation of self-standing hydrogels with solid-like mechanical properties ($G' > G''$), indicating that they would be above the gelation threshold, in agreement with what has been previously observed for similar sEPS hydrogels through phase diagrams [17]. According to these literature data [17], it is reasonable to suppose that, under the Ca^{2+} concentrations here applied, the minimum sEPS concentration above which the formation of a hydrogel network occurs would be close to 0.5 wt%. More in general, sEPS and M^{2+} concentration thresholds for hydrogel-formation can vary depending on the origin of microbial aggregates [17,24]. It is worth noting that, in previous works on AGS-derived sEPS hydrogels, a discontinuity in the slopes of the graphs plotting G' (or complex viscosity) vs. sEPS concentration was observed and ascribed to a concentration limit (about 2.5 wt% [24] – 4 wt% [23]), above which G' (or complex viscosity) more drastically increased. However, as shown in Fig. 5, this discontinuity was not here observed, likely due to the too low sEPS concentrations tested (< 2 wt %).

3.6. Practical implications

The main findings regarding the comparison between NaOH- and Na_2CO_3-based extractions are here interpreted within an integrated framework that brings together recoverability, fundamental characterization, profitability for biomaterial development and operational aspects. In this regard, Table 3 provides a concise summary of the main advantages and limitations of each tested protocol, highlighting key elements emerged from the comparative analysis. This focused overview not only helps to clarify the relative performance of the two extraction approaches but would also provide a basis for guiding future research into more applicative-oriented studies. The main practical constraints of the used NaOH-based protocol would be associated with the extraction process itself, and particularly with its lower recovery yield (Table 1). Since such reduced NaOH-induced extraction efficiency may have been due to the rapid decrease in pH during the biomass incubation period, the adoption of pH-controlled strategies could help to enhance treatment effectiveness. However, this approach would imply a more intensive dosage of chemicals, potentially increasing risks of polymer degradation and operative costs. Another critical aspect linked to the NaOH-based extraction was the relatively low solid-liquid separation efficiency by centrifugation, resulting in the recovery of more loosely structured sEPS (acidic) pellets with concentrations ≤1.9 wt%. This would represent a technical constraint for industrial facilities, which should employ coagulating/flocculating agents to enhance the sEPS separation efficiency after acidic treatment. As highlighted in Table 3, while Na_2CO_3-based extraction would appear more effective in terms of recovery yield and easier process operations, further considerations should be made regarding the resulting EPS/sEPS potential for product development. Indeed, the use of NaOH in the thermo-alkaline stage promoted the formation of stiffer sEPS hydrogels at relatively low sEPS concentrations (< 2 wt%) (Fig. 4), with profitable implications from an industrial valorization perspective. On the other hand, the Na_2CO_3-based protocol would allow to easily increase concentrations of sEPS

Table 3
Practical advantages and limitations associated with the NaOH- and Na_2CO_3-based protocols used in this study for the recovery of EPS/sEPS from AGS. It should be noticed that the considerations regarding the extraction process are specific to the experimental conditions here applied, particularly with respect to reagent dosage and pH (initial pH ~ 11.3; not controlled pH during the incubation period).

NaOH	
Advantages	Disadvantages
Feasibility of forming hydrogels with superior mechanical features at relatively low sEPS concentrations (≤ 1.9 wt%)	Lower extraction yield
	Loosely structured sEPS acidic pellets, resulting in a lower solid-liquid separation efficiency by centrifugation
	Impossibility of increasing the concentration (TS/WW mass ratio) of sEPS acidic pellets by centrifugation above about 1.9 wt%
	Lower content of high thermal resistant compounds
	Highly corrosive, requiring strict safety measures
Strong base likely leading to more intensive hydrolysis/partial degradation of specific EPS constituents	

Na_2CO_3	
Advantages	Disadvantages
Higher extraction yield	Formation of weaker hydrogels at relatively low sEPS concentrations (≤ 1.9 wt%)
Well-structured sEPS acidic pellets, leading to a higher solid-liquid separation efficiency by centrifugation	
Possibility of easily increasing the concentration (TS/WW mass ratio) of sEPS acidic pellets by centrifugation	
Feasibility of tailoring the hydrogel mechanics by playing with a wider range of sEPS concentrations	
Larger content of high thermal resistant compounds	
Less hazardous, easier to be handled and potentially more cost-effective	
Weaker base with a milder effect on the extractable EPS constituents	

extracts via centrifugation. Since a strong increase in the post-gelling stiffness is typically reported for sEPS concentrations higher than 2 wt % [23,24], the Na_2CO_3-based protocol would potentially enable the formation of even stiffer hydrogels by simply playing with a wider range of sEPS concentrations. In this perspective, the Na_2CO_3-based approach would favour an easier design of sEPS hydrogels with tunable rheological features. Moreover, the Na_2CO_3-based protocol would allow to extract more thermally resistant compounds that reasonably provide higher thermal stability to the recovered sEPS (Fig. 1), with potential benefits in the development of flame-retardant materials [12,36].

NaOH, being a strong base, is expected to induce more intensive hydrolysis/partial degradation of some EPS constituents (e.g. proteinaceous and lipidic fractions), reasonably altering the molecular weight profile (Table 2) and functional properties of the recovered biopolymers. The NaOH-based protocol would also limit the formation of supramolecular assemblies that are more prone to shear-induced deformation (i.e. lamellar structures). These phenomena could be advantageous in processes that require a sort of selective "purification" of EPS/sEPS extracts, especially when an improvement in the hydrogel mechanical features is requested. Conversely, Na_2CO_3 would exert milder chemical effects on the recoverable EPS constituents, thus helping to preserve their molecular weight distribution, structural arrangements, etc. Furthermore, considering the well-documented toxic effect of LPS associated with its Lipid A moiety [61–63], the fact that NaOH-based extraction may reduce the presence of LPS (and/or more intensively hydrolyze their lipidic portion) could likely contribute to a decrease in the potential toxicity of the extracted EPS/sEPS with respect to the Na_2CO_3-based protocol. Depending on the targeted EPS/sEPS valorization pathways, all the aspects highlighted above can contribute to the pros/cons analysis, again remarking the importance of fine-tuning the recovery processes according to application-related criteria.

When comparing the NaOH- and Na_2CO_3-based extractions, operational factors (Table 3) – together with life cycle and techno-economic considerations – should be also taken into account. NaOH is highly corrosive, thus requiring stringent safety measures and careful handling strategies, including the use of corrosion-resistant equipment. Conversely, Na_2CO_3 is less hazardous and might be hance associated with more efficient logistics due to the simpler storage and handling requirements, thus potentially contributing to more cost-effective chemical treatments. However, the higher base strength of NaOH could allow lower chemical dosages, potentially offsetting part of its life cycle and economic impacts depending on the specific application conditions. It is worth noting that the carbon footprint associated with the production of NaOH and Na_2CO_3 – which on industrial scale primarily involves chlor-alkali and Solvay processes, respectively – could vary depending on several factors, including energy source (fossil or renewable), electricity mix (especially for the electricity-intensive chlor-alkali process) and plant configuration [64–66]: thus, referring to both conventional and emerging technologies, these variables should be considered when comparing the NaOH and Na_2CO_3 life cycle impacts. All the aspects highlighted above should be carefully evaluated when the overall economic and environmental sustainability of the EPS/sEPS extraction process is addressed. Aware of the qualitative nature of the above considerations, dedicated life cycle assessment and techno-economic analysis studies will be strongly encouraged in future works to quantitatively assess the impacts of the proposed extraction processes. These analyses would provide a robust framework to identify trade-offs and optimization pathways, thus supporting the scalability of EPS/sEPS recovery processes in a technically feasible, economically viable and environmentally sustainable manner.

In summary, Na_2CO_3-based extractions would appear more suitable to balance high recovery yields and operational advantages (e.g. safety, handling, etc.), while exerting milder chemical effects on the extractable EPS/sEPS. However, considering the potential reference market for the recovered biopolymers, evaluations on a case-by-case basis should be made to support the design of more efficient EPS/sEPS production chains. The choice of chemicals and extraction conditions to be employed should be hence driven by techno-economic and environmental considerations, taking the specific requirements of the targeted applicative solution into account.

Beyond the practical implications related to the recovery process, the research findings of this study in terms of physicochemical, structural and rheological features also suggested valuable applicative potentials for the EPS/sEPS extracted with both NaOH- and Na_2CO_3-based protocols. The feasibility of forming hydrogel-like systems with tunable nano-scale architecture and mechanical properties would pave the way for the rational design of effective biomaterials in multiple valorization scenarios. Hydrogels that retain large quantities of water while maintaining solid-like rheological behavior could serve as carriers for controlled release of targeted compounds [17]. In this regard, they may be applied in the development of soil conditioners or agrochemical delivery systems, where the network strength protects encapsulated compounds from degradation and preserves hydrogel integrity over time, while the water-holding capacity contributes to improve soil hydration. The observed structural features coupled with scalable mechanical characteristics may support the use of EPS-based systems as rheology modifiers or thickeners [24]. Additionally, the abundance and availability of functional groups able to interact with (divalent) metal cations

could make these systems suitable as adsorbent media for the removal of targeted contaminants (such as many heavy metals) from wastewater [14,15]. While the above only outlines a selection of potential application-oriented strategies suggested by the observed physico-chemical and functional properties of the recovered biopolymers, it would provide a rationale for further exploring targeted valorization pathways towards more sustainable environmental and industrial solutions.

4. Conclusions

This work provided valuable insights into the complex nature of AGS-derived EPS/sEPS and related hydrogels, contributing to a novel, multi-scale perspective on their characterization under different (alkaline) recovery conditions. The main findings emerged from the comparative analysis of NaOH- and Na_2CO_3-based extraction protocols are summarized below.

i. EPS/sEPS recovery and composition

The NaOH-based extraction determined a significant reduction in the EPS recovery yield, reasonably influenced by the rapid decrease in pH during the incubation period. The NaOH-extracted sEPS exhibited a shift in the MW distribution towards smaller fractions. Conversely, the Na_2CO_3-based protocol provided better extraction performance, while enabling the recovery of larger and more thermally resistant polymers. These results suggested that the NaOH-based extraction likely induced more extensive hydrolysis/degradation of specific EPS components (e.g. proteinaceous fractions), while the Na_2CO_3-based alkaline stage had milder chemical effects on the recoverable EPS.

ii. Structural and mechanical features of sEPS hydrogels

SAXS measurements revealed that the sEPS hydrogel network likely consisted of 3D mass fractals and highly ordered lamellar, multilayered configurations – potentially attributable to LPS assemblies – which were more abundant in the case of Na_2CO_3-based extraction. Despite the higher degree of structural order, sEPS hydrogels from Na_2CO_3-based protocol exhibited reduced mechanical features. The NaOH-based extraction may have helped to purify sEPS extracts by more intensively hydrolyzing/degrading specific EPS constituents, such as large proteins and lipidic fractions, which may not significantly contribute to, or may even compromise, the hydrogel stiffness. The use of NaOH also limited the formation of supramolecular arrangements that more readily deform under shear (e.g. lamellar structures). These phenomena may therefore have contributed to an increase in the hydrogel stiffness for the NaOH-based protocol.

iii. Operational aspects

The use of NaOH could be associated with more stringent requirements in terms of safety measures, handling and storage, while potentially allowing lower dosages. Future life cycle and tecno-economic assessment studies are encouraged to frame NaOH- and Na_2CO_3-based extractions from an operational perspective.

The above highlighted the critical role of alkaline extraction in determining EPS/sEPS recovery yield and fundamental properties. The need for tunable recovery strategies was thus emphasized as pivotal for advancing knowledge of EPS/sEPS in both characterization- and application-oriented studies. Overall, this work would extend the current understanding of AGS-derived EPS systems, while providing a solid scientific base to guide future research into the rational design of effective biomaterials within the broader context of sustainable resource recovery.

CRediT authorship contribution statement

Benedetta Pagliaccia: Writing – review & editing, Writing – original draft, Visualization, Validation, Methodology, Investigation, Formal analysis, Data curation, Conceptualization. **Yuemei Lin:** Writing – review & editing, Visualization, Validation, Methodology, Investigation, Formal analysis, Data curation, Conceptualization. **Emiliano Carretti:** Writing – review & editing, Visualization, Validation, Methodology, Investigation, Formal analysis, Data curation, Conceptualization. **Lucrezia Caselli:** Writing – review & editing, Visualization, Validation, Methodology, Investigation, Formal analysis, Data curation. **Claudio Lubello:** Writing – review & editing, Supervision, Resources, Project administration, Funding acquisition. **Tommaso Lotti:** Writing – review & editing, Visualization, Validation, Supervision, Project administration, Methodology, Investigation, Formal analysis, Data curation, Conceptualization.

Declaration of competing interest

The authors declare that they have no known competing financial interests or personal relationships that could have appeared to influence the work reported in this paper.

Acknowledgements

This research was co-funded by the European Union - Next Generation EU. National Recovery and Resilience Plan (NRRP) – M4C2 Investment 1.3 - Research Program PE_00000005 “RETURN” - CUP B83C22004820002. Views and opinions expressed are however those of the author(s) only and do not necessarily reflect those of the European Union or the European Commission. Neither the European Union nor the European Commission can be held responsible for them.

The work was also financially supported by POR FESR Toscana 2014–2020, IDRO.SMART project (CUP: 3647.04032020.157000040).

Appendix A. Supplementary data

Supplementary data to this article can be found online at https://doi.org/10.1016/j.cej.2026.175798.

Data availability

Data will be made available on request.

References

[1] H.C. Flemming, J. Wingender, The biofilm matrix, Nat. Rev. Microbiol. 8 (2010) 623–633, https://doi.org/10.1038/nrmicro2415.
[2] G.P. Sheng, H.Q. Yu, X.Y. Li, Extracellular polymeric substances (EPS) of microbial aggregates in biological wastewater treatment systems: A review, Biotechnol. Adv. 28 (6) (2010) 882–894, https://doi.org/10.1016/j.biotechadv.2010.08.001.
[3] T. Seviour, N. Derlon, M.S. Dueholm, H.C. Flemming, E. Girbal-Neuhauser, H. Horn, S. Kjelleberg, M.C.M. van Loosdrecht, T. Lotti, M.F. Malpei, R. Nerenberg, T.R. Neu, E. Paul, H. Yu, Y. Lin, Extracellular polymeric substances of biofilms: Suffering from an identity crisis, Water Res. 151 (2019) 1–7, https://doi.org/10.1016/j.watres.2018.11.020.
[4] H.C. Flemming, E.D. van Hullebusch, B.J. Little, T.R. Neu, P.H. Nielsen, T. Seviour, P. Stoodley, J. Wingender, S. Wuertz, Microbial extracellular polymeric substances in the environment, technology and medicine, Nat. Rev. Microbiol. 23 (2025) 87–105, https://doi.org/10.1038/s41579-024-01098-y.
[5] S. Felz, P. Vermeulen, M.C.M. van Loosdrecht, Y. Lin, Chemical characterization methods for the analysis of structural extracellular polymeric substances (EPS), Water Res. 157 (2019) 201–208, https://doi.org/10.1016/j.watres.2019.03.068.
[6] S.A. Zahra, R. Persiani, M.K. Dueholm, M.C.M. van Loosdrecht, P.H. Nielsen, T. W. Seviour, Y. Lin, Rethinking characterization, application, and importance of extracellular polymeric substances in water technologies, Curr. Opin. Biotechnol. 89 (2024) 103192, https://doi.org/10.1016/j.copbio.2024.103192.
[7] M. Boleij, M. Pabst, T.R. Neu, M.C.M. Van Loosdrecht, Y. Lin, Identification of Glycoproteins Isolated from Extracellular Polymeric Substances of Full-Scale Anammox Granular Sludge, Environ. Sci. Technol. 52 (22) (2018) 13127–13135, https://doi.org/10.1021/acs.est.8b03180.

[8] P. Larsen, J.L. Nielsen, D. Otzen, P.H. Nielsen, Amyloid-like adhesins produced by floc-forming and filamentous bacteria in activated sludge, Appl. Environ. Microbiol. 74 (2008) 1517–1526, https://doi.org/10.1128/AEM.02274-07.

[9] T. Lotti, E. Carretti, D. Berti, C. Montis, S. Del Buffa, C. Lubello, C. Feng, F. Malpei, Hydrogels formed by anammox extracellular polymeric substances: structural and mechanical insights, Sci. Rep. 9 (2019) 11633, https://doi.org/10.1038/s41598-019-47987-8.

[10] D.R. de Graaff, S. Felz, T.R. Neu, M. Pronk, M.C.M. van Loosdrecht, Y. Lin, Sialic acids in the extracellular polymeric substances of seawater-adapted aerobic granular sludge, Water Res. 155 (2019) 343–351, https://doi.org/10.1016/j.watres.2019.02.040.

[11] S. Felz, T.R. Neu, M.C.M. van Loosdrecht, Y. Lin, Aerobic granular sludge contains Hyaluronic acid-like and sulfated glycosaminoglycans-like polymers, Water Res. 169 (2020) 115291, https://doi.org/10.1016/j.watres.2019.115291.

[12] N.K. Kim, N. Mao, R. Lin, D. Bhattacharyya, M.C.M. van Loosdrecht, Y. Lin, Flame retardant property of flax fabrics coated by extracellular polymeric substances recovered from both activated sludge and aerobic granular sludge, Water Res. 170 (2020) 115344, https://doi.org/10.1016/j.watres.2019.115344.

[13] Y. Lin, K.G.J. Nierop, E. Girbal-Neuhauser, M. Adriaanse, M.C.M. van Loosdrecht, Sustainable polysaccharide-based biomaterial recovered from waste aerobic granular sludge as a surface coating material, Sustain, Mater. Technol. 4 (2015) 24–29, https://doi.org/10.1016/j.susmat.2015.06.002.

[14] N. Li, D. Wei, S. Wang, L. Hu, W. Xu, B. Du, Q. Wei, Comparative study of the role of extracellular polymeric substances in biosorption of Ni(II) onto aerobic/anaerobic granular sludge, J. Colloid Interface Sci. 490 (2017) 754–761, https://doi.org/10.1016/j.jcis.2016.12.006.

[15] B. Pagliaccia, E. Carretti, M. Severi, D. Berti, C. Lubello, T. Lotti, Heavy metal biosorption by Extracellular Polymeric Substances (EPS) recovered from anammox granular sludge, J. Hazard. Mater. 424 (2022) 126661, https://doi.org/10.1016/j.jhazmat.2021.126661.

[16] N.P. Amin Vieira da Costa, N. Libardi, R.H. Ribeiro da Costa, How can the addition of extracellular polymeric substances (EPS)-based bioflocculant affect aerobic granular sludge (AGS)? J. Environ. Manag. 310 (2022) 114807 https://doi.org/10.1016/j.jenvman.2022.114807.

[17] B. Pagliaccia, R. Campo, E. Carretti, M. Severi, C. Lubello, T. Lotti, Towards resource recovery-oriented solutions in agriculture exploiting structural extracellular polymeric substances (sEPS) extracted from aerobic granular sludge (AGS), Chem. Eng. J. 485 (2024) 149819, https://doi.org/10.1016/j.cej.2024.149819.

[18] I. Karakas, S.B. Sam, E. Cetin, E. Dulekgurgen, G. Yilmaz, Resource recovery from an aerobic granular sludge process treating domestic wastewater, J. Water Process Eng. 34 (2020) 101148, https://doi.org/10.1016/j.jwpe.2020.101148.

[19] M. Pronk, M.K. de Kreuk, B. de Bruin, P. Kamminga, R. Kleerebezem, M.C.M. van Loosdrecht, Full scale performance of the aerobic granular sludge process for sewage treatment, Water Res. 84 (2015) 207–217, https://doi.org/10.1016/j.watres.2015.07.011.

[20] R. Campo, S. Sguanci, S. Caffaz, L. Mazzoli, M. Ramazzotti, C. Lubello, T. Lotti, Efficient carbon, nitrogen and phosphorus removal from low C/N real domestic wastewater with aerobic granular sludge, Bioresour. Technol. 305 (2020) 122961, https://doi.org/10.1016/j.biortech.2020.122961.

[21] N.M. Pfaff, J.A. Dijksman, A.J.B. Kemperman, M.C.M. van Loosdrecht, J.M. Kleijn, Rheological characterisation of alginate-like exopolymer gels crosslinked with calcium, Water Res. 207 (2021) 117835, https://doi.org/10.1016/j.watres.2021.117835.

[22] S. Felz, S. Al-Zuhairy, O.A. Aarstad, M.C.M. van Loosdrecht, Y. Lin, Extraction of structural extracellular polymeric substances from aerobic granular sludge, J. Vis. Exp. 115 (2016) e54534, https://doi.org/10.3791/54534.

[23] R. Campo, E. Carretti, C. Lubello, T. Lotti, Recovery of structural extracellular polymeric substances (sEPS) from aerobic granular sludge: Insights on biopolymers characterization and hydrogel properties for potential applications, J. Environ. Manag. 324 (2022) 116247, https://doi.org/10.1016/j.jenvman.2022.116247.

[24] B. Pagliaccia, S. Durieux, Y. Bessiere, M. Bounouba, A. Bou-Sarkis, E. Girbal-Neuhauser, E. Carretti, C. Lubello, T. Lotti, E. Paul, Insights on the hydrogel-forming ability and post-gelling mechanical properties of structural extracellular polymeric substances (sEPS) from aerobic granular sludge (AGS): A comparison with model biopolymers, J. Water Process Eng. 49 (2022) 103076, https://doi.org/10.1016/j.jwpe.2022.103076.

[25] S. Felz, H. Kleikamp, J. Zlopasa, M.C.M. van Loosdrecht, Y. Lin, Impact of metal ions on structural EPS hydrogels from aerobic granular sludge, Biofilm 2 (2020) 100011, https://doi.org/10.1016/j.bioflm.2019.100011.

[26] Y. Lin, P.K. Sharma, M.C.M. van Loosdrecht, The chemical and mechanical differences between alginate-like exopolysaccharides isolated from aerobic flocculent sludge and aerobic granular sludge, Water Res. 47 (1) (2013) 57–65, https://doi.org/10.1016/j.watres.2012.09.017.

[27] J. Li, X. Hao, M.C.M. van Loosdrecht, Y. Lin, Understanding the ionic hydrogel-forming property of extracellular polymeric substances: Differences in lipopolysaccharides between flocculent and granular sludge, Water Res. 268 (2025) 122707, https://doi.org/10.1016/j.watres.2024.122707.

[28] C.M. Schambeck, E. Girbal-Neuhauser, L. Böni, P. Fischer, Y. Bessière, E. Paul, R.H. R. da Costa, N. Derlon, Chemical and physical properties of alginate-like exopolymers of aerobic granules and flocs produced from different wastewaters, Bioresour. Technol. 312 (2020) 123632, https://doi.org/10.1016/j.biortech.2020.123632.

[29] A. Bou-Sarkis, B. Pagliaccia, A. Ric, N. Derlon, E. Paul, Y. Bessiere, E. Girbal-Neuhauser, Effects of alkaline solvents and heating temperatures on the solubilization and degradation of gel-forming Extracellular Polymeric Substances (EPS) extracted from aerobic granular sludge, Biochem. Eng. J. 185 (2022) 108500, https://doi.org/10.1016/j.bej.2022.108500.

[30] P. D'Abzac, F. Bordas, E. Van Hullebusch, P.N.L. Lens, G. Guibaud, Extraction of extracellular polymeric substances (EPS) from anaerobic granular sludges: comparison of chemical and physical extraction protocols, Appl. Microbiol. Biotechnol. 85 (2010) 1589–1599, https://doi.org/10.1007/s00253-009-2288-x.

[31] X. Xu, L. Zhang, X. Zhang, X. Guan, D. Wei, Effect of Mn^{2+} on the phosphorus removal and bioflocculation under anoxic condition, J. Environ. Sci. 115 (2022) 37–46, https://doi.org/10.1016/j.jes.2021.07.012.

[32] X. Xu, J. Zhong, X. Hao, Q. Liu, M. Lu, X. Guan, L. Zhang, Migration and morphological transformation of Mn^{2+} and its effect on microbial community in the A^2O process, J. Environ. Sci. 157 (2025) 404–416, https://doi.org/10.1016/j.jes.2024.11.015.

[33] C. Feng, T. Lotti, Y. Lin, F. Malpei, Extracellular polymeric substances extraction and recovery from anammox granules: Evaluation of methods and protocol development, Chem. Eng. J. 374 (2019) 112–122, https://doi.org/10.1016/j.cej.2019.05.127.

[34] M.L. Sesay, G. Özcengiz, F.D. Sanin, Enzymatic extraction of activated sludge extracellular polymers and implications on bioflocculation, Water Res. 40 (7) (2006) 1359–1366, https://doi.org/10.1016/j.watres.2006.01.045.

[35] B. Ou, X. Hu, W. Yu, F. Meng, W. Li, S. Liang, S. Yuan, H. Duan, H. Hou, K. Xiao, Critical evaluation of extracellular polymeric substances extraction methods: Extraction efficiency, molecular characteristics, and heavy metals binding properties, Sci. Total Environ. 959 (2025) 178345, https://doi.org/10.1016/j.scitotenv.2024.178345.

[36] T.M. Le, Y. Lin, W.Q. Zhuang, K. Jayaraman, N.K. Kim, Effects of Extraction Methods on the Thermal Stability of Extracellular Polymeric Substances-Based Biomaterials from Wastewater Sludge, Environ. Sci. Technol. 59 (8) (2025) 4165–4177, https://doi.org/10.1021/acs.est.4c10329.

[37] APHA/AWWA/WEF, Standard methods for the examination of water and wastewater, 23rd ed, American Public Health Association, Washington, DC, USA, 2017.

[38] L.M. Chen, S. de Bruin, M. Pronk, D.Z. Sousa, M.C.M. van Loosdrecht, Y. Lin, Sialylation and Sulfation of Anionic Glycoconjugates Are Common in the Extracellular Polymeric Substances of Both Aerobic and Anaerobic Granular Sludges, Environ. Sci. Technol. 57 (35) (2023) 13217–13225, https://doi.org/10.1021/acs.est.2c09586.

[39] S. Manioglu, S.M. Modaresi, N. Ritzmann, J. Thoma, S.A. Overall, A. Harms, G. Upert, A. Luther, A.B. Barnes, D. Obrecht, D.J. Müller, S. Hiller, Antibiotic polymyxin arranges lipopolysaccharide into crystalline structures to solidify the bacterial membrane, Nat. Commun. 13 (2022) 6195, https://doi.org/10.1038/s41467-022-33838-0.

[40] T. Narayanan, M. Sztucki, P. Van Vaerenbergh, J. Léonardon, J. Gorini, L. Claustre, F. Sever, J. Morse, P. Boesecke, A multipurpose instrument for time-resolved ultra-small-angle and coherent X-ray scattering, J. Appl. Crystallogr. 51 (2018) 1511–1524, https://doi.org/10.1107/S1600576718012748.

[41] T. Lotti, E. Carretti, D. Berti, M.R. Martina, C. Lubello, F. Malpei, Extraction, recovery and characterization of structural extracellular polymeric substances from anammox granular sludge, J. Environ. Manag. 236 (2019) 649–656, https://doi.org/10.1016/j.jenvman.2019.01.054.

[42] F. Hou, W. Ding, W. Qu, A.O. Oladejo, F. Xiong, W. Zhang, R. He, H. Ma, Alkali solution extraction of rice residue protein isolates: Influence of alkali concentration on protein functional, structural properties and lysinoalanine formation, Food Chem. 218 (2017) 207–215, https://doi.org/10.1016/j.foodchem.2016.09.064.

[43] X. Li, S. Lin, T. Hao, S.K. Khanal, G. Chen, Elucidating pyrolysis behaviour of activated sludge in granular and flocculent form: Reaction kinetics and mechanism, Water Res. 162 (2019) 409–419, https://doi.org/10.1016/j.watres.2019.06.074.

[44] J. Zhang, W. Song, Y. Zhong, D. Wang, Y. Deng, Extraction, structural characteristics and antioxidant activity of hemp seeds glycoprotein, Food Sci. Biotechnol. 33 (2024) 3553–3565, https://doi.org/10.1007/s10068-024-01583-3.

[45] L. Yun, S. Wang, T. Wu, Q. Li, M. Zhang, Structural characterization of a novel glycoprotein in wheat germ and its physicochemical properties, Int. J. Biol. Macromol. 117 (2018) 1058–1065, https://doi.org/10.1016/j.ijbiomac.2018.05.169.

[46] A. Zacheo, L. Bizzarro, L. Blasi, C. Piccirillo, A. Cardone, G. Gigli, A. Ragusa, A. Quarta, Lipid-Based Nanovesicles for Simultaneous Intracellular Delivery of Hydrophobic, Hydrophilic, and Amphiphilic Species, Front. Bioeng. Biotechnol. 8 (2020) 690, https://doi.org/10.3389/fbioe.2020.00690.

[47] J. Naktiyok, H. Bayrakçeken, A.K. Özer, M.Ş. Gülaboğlu, Kinetics of thermal decomposition of phospholipids obtained from phosphate rock, Fuel Process. Technol. 116 (2013) 158–164, https://doi.org/10.1016/j.fuproc.2013.05.007.

[48] M.C. Ramos-Sánchez, A. Rodríguez-Torres, J.A. Leal, F.J. Martín-Gil, J. Martín-Gil, Thermolytical Techniques To Characterize Fungal Polysaccharides and Bacterial Lipopolysaccharides, Biotechnol. Prog. 7 (6) (1991) 526–533, https://doi.org/10.1021/bp00012a007.

[49] L. Caselli, L. Conti, I. De Santis, D. Berti, Small-angle X-ray and neutron scattering applied to lipid-based nanoparticles: Recent advancements across different length scales, Adv. Colloid Interf. Sci. 327 (2024) 103156, https://doi.org/10.1016/j.cis.2024.103156.

[50] L.A. Feigin, D.I. Svergun, Structure Analysis by Small-Angle X-Ray and Neutron Scattering, Plenum Press, New York, 1987.

[51] G. Ochbaum, R. Bitton, 14 - Using small-angle X-ray scattering (SAXS) to study the structure of self-assembling biomaterials, in: H.S. Azevedo, R.M.P. da Silva (Eds.), Self-Assembling Biomaterials, Woodhead Publishing, 2018, pp. 291–304, https://doi.org/10.1016/B978-0-08-102015-9.00015-0.

[52] D. Stauffer, A. Aharony, Introduction To Percolation Theory, Second Edition (2nd ed.), Taylor & Francis, London, 1992, https://doi.org/10.1201/9781315274386.
[53] G. Evmenenko, E. Theunissen, K. Mortensen, H. Reynaers, SANS study of surfactant ordering in k-carrageenan/cetylpyridinium chloride complexes, Polymer 42 (7) (2001) 2907–2913, https://doi.org/10.1016/S0032-3861(00)00674-1.
[54] K. Almdal, J. Dyre, S. Hvidt, O. Kramer, Towards a phenomenological definition of the term 'gel,', Polym. Gels Netw. 1 (1) (1993) 5–17, https://doi.org/10.1016/0966-7822(93)90020-I.
[55] T. Seviour, M. Pijuan, T. Nicholson, J. Keller, Z. Yuan, Understanding the properties of aerobic sludge granules as hydrogels, Biotechnol. Bioeng. 102 (5) (2009) 1483–1493, https://doi.org/10.1002/bit.22164.
[56] T. Seviour, M. Pijuan, T. Nicholson, J. Keller, Z. Yuan, Gel-forming exopolysaccharides explain basic differences between structures of aerobic sludge granules and floccular sludges, Water Res. 43 (18) (2009) 4469–4478, https://doi.org/10.1016/j.watres.2009.07.018.
[57] S. Mistry, P.L. Fuhrmann, A. de Vries, R. Karshafian, D. Rousseau, Structure-rheology relationship in monoolein liquid crystals, J. Colloid Interface Sci. 630 (2023) 878–887, https://doi.org/10.1016/j.jcis.2022.10.115.
[58] P.G. De Gennes, On a relation between percolation theory and the elasticity of gels, J. Physique Lett. 37 (1976) 1–2, https://doi.org/10.1051/jphyslet:019760037010100.
[59] D. Stauffer, Gelation in concentrated critically branched polymer solutions. Percolation scaling theory of intramolecular bond cycles, J. Chem. Soc. Faraday Trans. II (72) (1976) 1354–1364, https://doi.org/10.1039/F29767201354.
[60] J.M. Guenet, Structure versus rheological properties in fibrillar thermoreversible gels from polymers and biopolymers, J. Rheol. 44 (2000) 947–960, https://doi.org/10.1122/1.551121.
[61] U. Seydel, L. Hawkins, A.B. Schromm, H. Heine, O. Scheel, M.H.J. Koch, K. Brandenburg, The generalized endotoxic principle, Eur. J. Immunol. 33 (6) (2003) 1586–1592, https://doi.org/10.1002/eji.200323649.
[62] H. Takada, S. Kotani, O. Lüderitz, Structural Requirements of Lipid a for Endotoxicity and Other Biological Activities, CRC Crit. Rev. Microbiol. 16 (6) (1989) 477–523, https://doi.org/10.3109/10408418909104475.
[63] A. Molinaro, O. Holst, F. Di Lorenzo, M. Callaghan, A. Nurisso, G. D'Errico, A. Zamyatina, F. Peri, R. Berisio, R. Jerala, J. Jiménez-Barbero, A. Silipo, S. Martín-Santamaría, Chemistry of Lipid A: At the Heart of Innate Immunity, Chem. Eur. J. 21 (2) (2015) 500–519, https://doi.org/10.1002/chem.201403923.
[64] I. Garcia-Herrero, M. Margallo, R. Onandía, R. Aldaco, A. Irabien, Environmental challenges of the chlor-alkali production: Seeking answers from a life cycle approach, Sci. Total Environ. 580 (2017) 147–157, https://doi.org/10.1016/j.scitotenv.2016.10.202.
[65] E. Medina-Martos, J.L. Gálvez-Martos, J. Almarza, C. Lirio, D. Iribarren, A. Valente, J. Dufour, Environmental and economic performance of carbon capture with sodium hydroxide, J. CO_2 Util. 60 (2022) 101991, https://doi.org/10.1016/j.jcou.2022.101991.
[66] A. Baral, J.L. Galvez-Martos, T. Hanein, Realizing CO_2 emission reduction in lime and soda ash manufacturing through anion exchange, Green Chem. 27 (2025) 3431–3442, https://doi.org/10.1039/d4gc05568c.